

UNCLASSIFIED

AD NUMBER

ADB007226

LIMITATION CHANGES

TO:

Approved for public release; distribution is unlimited.

FROM:

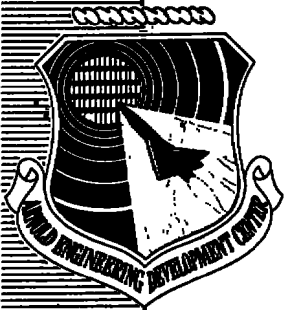
Distribution authorized to U.S. Gov't. agencies only; Test and Evaluation; OCT 1975. Other requests shall be referred to Space and Missile Systems Organization, PO box 92960, Los Angeles, CA 90009.

AUTHORITY

SAMSO ltr 29 Nov 1976

THIS PAGE IS UNCLASSIFIED

cy.2



ALTITUDE QUALIFICATION TEST OF THE AEROJET SVM-6 SOLID-PROPELLANT ROCKET MOTOR

ENGINE TEST FACILITY
ARNOLD ENGINEERING DEVELOPMENT CENTER
AIR FORCE SYSTEMS COMMAND
ARNOLD AIR FORCE STATION, TENNESSEE 37389

October 1975

Final Report for Period May 23 — June 20, 1975

This document has been prepared for public release

SAMS/USAF Ltr.
29 Nov 76

see TAB 77-6 (18 Mar 1977)

Distribution limited to U.S. Government agencies only; this report contains information on test and evaluation of military hardware; October 1975; other requests for this document must be referred to Space and Missile Systems Organization (SKI), PO Box 92960, WWPO, Los Angeles, California 90009.

Prepared for

SPACE AND MISSILE SYSTEMS ORGANIZATION (SKI)
P.O. BOX 92960, WWPO
LOS ANGELES, CALIFORNIA 90009

NOTICES

When U. S. Government drawings specifications, or other data are used for any purpose other than a definitely related Government procurement operation, the Government thereby incurs no responsibility nor any obligation whatsoever, and the fact that the Government may have formulated, furnished, or in any way supplied the said drawings, specifications, or other data. is not to be regarded by implication or otherwise, or in any manner licensing the holder or any other person or corporation, or conveying any rights or permission to manufacture, use, or sell any patented invention that may in any way be related thereto.

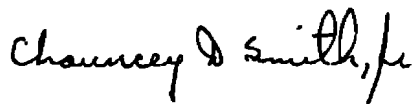
Qualified users may obtain copies of this report from the Defense Documentation Center.

References to named commercial products in this report are not to be considered in any sense as an endorsement of the product by the United States Air Force or the Government.

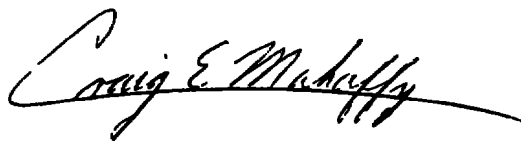
APPROVAL STATEMENT

This technical report has been reviewed and is approved for publication.

FOR THE COMMANDER



CHAUNCEY D. SMITH, JR.
Lt Colonel, USAF
Chief Air Force Test Director, ETF
Directorate of Test



CRAIG E. MAHAFFY
Colonel, USAF
Director of Test

UNCLASSIFIED

DD FORM 1473 EDITION OF 1 NOV 65 IS OBSOLETE

UNCLASSIFIED

UNCLASSIFIED

20. ABSTRACT (Continued)

performance, altitude ignition characteristics, motor temperature-time history, structural integrity of the motor, and the lateral (nonaxial) component of the thrust vector are presented and discussed.

UNCLASSIFIED

PREFACE

The test program reported herein was conducted by the Arnold Engineering Development Center (AEDC), Air Force Systems Command (AFSC), at the request of the Space and Missile Systems Organization (SAMSO), AFSC, for the Aerojet Solid Propulsion Company, under Program Element 02001D. The results were obtained by ARO, Inc. (a subsidiary of Sverdrup & Parcel and Associates, Inc.), contract operator of the AEDC, AFSC, Arnold Air Force Station, Tennessee. The tests were conducted in Propulsion Development Test Cell (T-3) of the Engine Test Facility (ETF) on May 23 and June 20, 1975, under ARO Project No. R41C-26A. The authors of this report were H. L. Merryman and L. R. Smith, ARO, Inc. The data analysis was completed on July 2, 1975, and the manuscript (ARO Control No. ARO-ETF-TR-75-135) was submitted for publication on September 5, 1975.

CONTENTS

	<u>Page</u>
1.0 INTRODUCTION	5
2.0 APPARATUS	5
3.0 PROCEDURE	7
4.0 RESULTS AND DISCUSSION	9
5.0 SUMMARY OF RESULTS	11
REFERENCES	12

ILLUSTRATIONS

Figure

1. Aerojet SVM-6 Solid-Propellant Rocket Motor	13
2. Installation of the Aerojet SVM-6 Rocket Motor in Propulsion Development Test Cell (T-3)	15
3. Instrumentation Locations	19
4. Variation in Thrust, Chamber Pressure, and Cell Pressure during Firing	21
5. Postfire Photographs of the Motor Assembly	22
6. Forward Dome Axial Growth Relative to Aft Skirt Attachment Ring	27
7. Motor Temperature Variation with Time	28
8. Variation in the Lateral (Nonaxial) Component of the Thrust Vector during Firing	38

TABLES

1. Instrumentation Summary and Measurement Uncertainty	40
2. Summary of SVM-6 Motor Performance	41
3. Summary of SVM-6 Motor Physical Dimensions	42
NOMENCLATURE	43

1.0 INTRODUCTION

The Aerojet SVM-6 solid-propellant rocket motor was designed to provide the orbit insertion thrust for the 1,530-lbm NATO III Satellite System. The SVM-6 Qualification Test Requirements (Ref. 1) include the firing of three motors at simulated altitude conditions to ensure that the motors conform to the specifications outlined in Ref. 2.

The results of the initial qualification firing for motor S/N Q-1 are contained in Refs. 3 and 4. The results of the second and third qualification firing are reported herein. The motors were preconditioned to temperatures of 110°F (S/N Q2) and 10°F (S/N Q3) and successfully fired at an ignition pressure altitude in excess of 100,000 ft while spinning at 110 rpm.

Motor altitude ballistic performance, altitude ignition characteristics, temperature-time history, component structural integrity, and the lateral (nonaxial) thrust data are presented and, where applicable, compared with the motor specification requirements (Ref. 2).

2.0 APPARATUS

2.1 TEST ARTICLE

The Aerojet SVM-6 solid-propellant rocket motor (Fig. 1) is a full-scale, flightweight motor with an overall length of 54 in. and diameter of 30 in. The loaded motor weight is nominally 800 lbm, of which 710 lbm is propellant.

The chamber assembly consists of a glass-filament-wound pressure vessel with an integral aluminum attachment ring and aluminum polar bosses to which the igniter and nozzle are bolted. The chamber assembly is internally insulated with molded silica-filled Buna-N rubber.

The case-bonded propellant grain consists of a thermally cured polybutadiene propellant designated ANB-3066. The internal grain configuration consists of an upstream cylindrical bore which diverges conically in the aft chamber.

The contoured nozzle assembly has a nominal throat area of 6.3 in.² and a 53:1 expansion ratio. The throat insert is fabricated from silver-infiltrated tungsten to minimize erosion.

The igniter assembly is installed in the forward dome polar boss and uses boron-potassium-nitrate pellets as the pyrotechnic charge. The primary charge consists of 10 gm of pellets, and the main charge contains 210 gm of pellets. The igniter incorporates a safe-arm-device which provides the first element of the ignition train; two independently activated US Flare ES-003 squibs are energized with 4.3 to 10.0 amp of direct current.

2.2 INSTALLATION

Each motor assembly was cantilever mounted from the spindle face of the spin fixture assembly in Propulsion Development Test Cell (T-3) (Fig. 2). The spin assembly was mounted on a thrust cradle, which was supported from the cradle support stand by three vertical and two horizontal double-flexure columns (Fig. 2d). The spin-fixture assembly consists of a 10-hp squirrel-cage-type drive motor, a thrust bearing assembly, and a 46-in.-long spindle having a 36-in.-diam aft spindle face. The spin fixture rotated counterclockwise, looking upstream. Electrical leads to and from the igniter and instrumentation systems on the rotating motor were routed through a 170-channel slipring assembly mounted between the forward and aft bearing assemblies of the spindle. Axial thrust was transmitted through the spindle thrust bearing to two double-bridge strain-gage-type load cells mounted just forward of the thrust bearing on the motor axial centerline.

Preignition pressure altitude conditions were maintained in the test cell by a steam ejector operating in series with the ETF exhaust gas compressors. During the motor firings, the motor exhaust gases were used as the driving gas for the 24-in.-diam. water-cooled ejector-diffuser system to maintain test cell pressure at an acceptable level.

2.3 INSTRUMENTATION

Instrumentation was provided to measure axial force, motor chamber pressure, lateral (nonaxial) force, test cell pressure, motor case and nozzle temperatures, motor forward dome linear growth, and motor rotational speed. Table 1 presents instrument ranges, recording methods, and measurement uncertainty for all reported parameters.

The axial force measuring system consisted of two double-bridge, strain-gage-type load cells mounted in the axial double-flexure column forward of the thrust bearing on the motor centerline. The lateral (nonaxial) force measuring system consisted of two double-bridge, strain-gage-type load cells installed forward and aft between the flexure-mounted cradle and the cradle support stand normal to and in the horizontal plane containing the motor axial centerline (Fig. 2d).

Unbonded strain-gage-type transducers were used to measure test cell pressure. Motor chamber pressure was measured with a 0- to 1,000-psia bonded strain-gage-type transducer teed with a 0- to 1,000-psia user-furnished flight-type transducer which is a part of the motor/spacecraft system. Chromel®-Alumel® (CA) thermocouples were bonded to the motor case and nozzle (Fig. 3) to measure surface temperatures during and after motor burn time. Motor forward dome growth was measured with a linear potentiometer installed between the motor mounting fixture and forward dome polar boss. Rotational speed of the motor assembly was determined from the output of a magnetic pickup.

The output signal of each measuring device was recorded on independent instrumentation channels. The four axial thrust channels, three test cell pressure channels, motor chamber growth, and two motor chamber pressure channels were recorded as follows: The millivolt outputs of the axial thrust load cells, chamber pressure transducers, and cell pressure transducers were recorded on magnetic tape from a multi-input, analog-to-digital converter and reduced to engineering units by an electronic computer. The computer provided a tabulation of average absolute values at 0.02-sec time increments and total integrals over the cumulative time increments.

Selected channels of thrust and pressures were recorded on null-balance, potentiometer-type strip charts for analysis immediately after the motor firing. Visual observation of the firing was provided by a closed-circuit television monitor. High-speed, motion-picture cameras provided a permanent visual record of the firing.

2.4 CALIBRATION

The thrust system calibrator weights, thrust load cells, and pressure transducers were laboratory calibrated prior to usage in this test. After installation of the measuring devices in the test cell, the devices were again calibrated at sea-level, non-spin, ambient conditions. The thrust load cells were calibrated at simulated altitude with the motor spinning at 110 rpm.

The pressure recording systems were calibrated by an electrical, four-step calibration using resistances in the transducer circuits to simulate selected pressure levels. The axial thrust instrumentation systems were calibrated by applying to the thrust cradle known forces, which were produced by deadweights acting through a bell crank. The calibrator is hydraulically actuated and remotely operated from the control room. Thermocouple recording instruments were calibrated by using millivolt levels to simulate thermocouple outputs. Nonlinearity in thermocouple characteristics was accounted for in the data reduction program.

After the motor firing, with the test cell still at simulated altitude pressure, the recording systems were recalibrated to determine any shift.

Calibrations of the lateral (nonaxial) force measuring system were conducted using the procedure outlined in Ref. 5.

3.0 PROCEDURE

The Aerojet SVM-6 motors were received at the AEDC on May 12 (S/N Q2) and May 27 (S/N Q3), 1975. The motors were visually inspected for possible shipping damage and radiographically inspected for grain cracks, voids, or separations. Neither motor

complied with the motor manufacturer's radiographic inspection criteria due to fiber glass case-to-insulation separation on each motor. Also the propellant trim on S/N Q3 had a maximum length of 4.188 in. which is greater than the 3.60 in. maximum allowable. The surface trim on the motor was an intentional removal of propellant, accomplished at the Aerojet facility as a means of balancing the motor.

The fiber glass case-to-insulation separation on motor S/N Q2 was a maximum of 1.188 in. long and 0.031 in. deep and extended 50 deg around the case. The separation on Q3 was a maximum of 0.625 in. long and 0.031 in. deep and extended 15 deg around the case. The radiographic criteria requires the motors to be free of unbondedness between insulation and all other appropriate components.

The discrepancies were discussed with Aerojet personnel and the following results obtained: (1) the out of tolerance trim would not be detectable on motor burning characteristics and (2) the area of case-to-insulation separation on each motor would not affect motor performance. Therefore, each motor was considered acceptable for test, and the subject radiographic criteria requirements were waived.

After radiographic inspection, the motors were stored in an area temperature conditioned at $70 \pm 5^{\circ}\text{F}$ where the motors were checked to ensure correct fit of mating hardware, and thermocouples were bonded to the motor case and nozzle. The nozzle throat and exit diameters were measured. After the motor was secured to the thrust adapter, the assembly was mounted on a spin table, and radial dimensions of selected surfaces were measured as a function of angular position relative to the centerline of the assembly to facilitate alignment with the spin rig axis during test cell installation. The entire assembly was then weighed and photographed.

After installation of each motor assembly in the test cell, the motor centerline was aligned with the spin rig spin axis, instrumentation connections were completed, and the motor assembly was balanced at 110 rpm. During the 72-hr period preceding the motor firing, test cell temperature was maintained at $110 \pm 5^{\circ}\text{F}$ (S/N Q2) and $10 \pm 5^{\circ}\text{F}$ (S/N Q3).

Motor Q3 was installed in a cryoplate assembly (Fig. 2c) through which cooled trichloroethylene was circulated to provide the desired thermal environment of $10 \pm 5^{\circ}\text{F}$. The space between the cryoplates and the motor case was purged with cold, dry gaseous nitrogen to remove water vapor which could have condensed as frost on the plate internal

surfaces. The $110 \pm 5^\circ\text{F}$ environment required for motor Q2 was maintained using the standard T-3 temperature-conditioning system.

The final operation prior to firing was to adjust the firing circuit resistance to provide a firing current to the igniter of 10 amp. The entire instrumentation measuring-recording complex was activated, and the motors were fired at simulated ignition altitudes of 113,000 ft (S/N Q2) and 123,000 ft (S/N Q3) while spinning at 110 rpm.

Spinning was continued for approximately 60 min after burnout during which time postfire calibrations were accomplished; motor temperatures were recorded continuously for 220 sec after ignition and then at 30 sec intervals until 20 min after burnout. The assembly was decelerated, slowly, until rotation had stopped, and another set of calibrations was taken. Test cell pressure was then returned to ambient conditions, and the motor assembly was inspected, photographed, and removed to the storage area where the nozzle throat and exit diameters and motor weight were measured, and the postfire condition of each motor was photographically recorded.

4.0 RESULTS AND DISCUSSION

Two Aerojet SVM-6 solid-propellant rocket motors (S/N's Q2 and Q3) were fired at ignition pressure altitudes of 113,000 and 123,000 ft, respectively, while spinning about their axial centerlines at 110 rpm as the final part of the SVM-6 qualification program. Prior to firing, the motors were preconditioned to a temperature of 110°F (S/N Q2) and 10°F (S/N Q3).

The program objectives were to determine vacuum ballistic performance, altitude ignition characteristics, motor temperature-time history, structural integrity of motor components and the lateral (nonaxial) component of the thrust vector. The applicable data were used to demonstrate compliance with motor specification (Ref. 2).

Altitude ignition characteristics and vacuum ballistic performance are presented in Table 2 and motor pre- and postfire physical measurements are summarized in Table 3. A temperature-time history of the motor cases and nozzles is presented and discussed. When multiple channels of equal accuracy instrumentation were used to obtain values of a single parameter, the average values were used to calculate the data presented.

4.1 ALTITUDE IGNITION CHARACTERISTICS AND BALLISTIC PERFORMANCE

The motors were successfully ignited at a pressure altitude of 113,000 (S/N Q2) and 123,000 ft (S/N Q3). The average pressures altitudes over action time were 82,000 ft (S/N Q2) and 83,000 ft (S/N Q3). Ignition time, the interval from firing current application to the time when thrust reaches 75 percent of maximum ignition thrust, was

0.013 sec for motor S/N Q2 and 0.038 sec for motor S/N Q3, which is in conformance with the 0.185 sec maximum specified in Ref. 2.

The variations in measured thrust, chamber pressure, and test cell pressure during each firing are presented in Fig. 4. Total burn times were 35.905 and 40.578 sec for Q2 and Q3, respectively. Action times, the interval between 10 percent of maximum chamber pressure during ignition to 10 percent of maximum pressure during tailoff, were 29.037 and 34.353 sec for Q2 and Q3, respectively. This is in conformance with Ref. 2 which states that action time is not to exceed 43 sec (at 55°F).

Vacuum total impulse values were 208,433 lbf-sec (S/N Q2) and 208,474 lbf-sec (S/N Q3). Reference 2 states that the vacuum total impulse is to be within 0.75 percent of 210,000 lbf-sec (or from 208,425 to 211,575 lbf-sec). Therefore, the vacuum total impulse of both motors conformed to the specification requirements. Vacuum total impulse uncertainties in percent of reading were ± 0.2444 and ± 0.2520 percent for motors Q2 and Q3, respectively.

The vacuum specific impulse values based on the manufacturer's stated propellant weight and total burn time (t_T), were 294.97 and 293.72 lbf-sec/lbm for motors Q2 and Q3, respectively. Vacuum specific impulse values based on expended mass (measured at AEDC) and t_T were 291.20 and 289.77 lbf-sec/lbm for motors Q2 and Q3, respectively. Vacuum specific impulse uncertainties in percent of reading were ± 0.2468 and ± 0.2542 percent for motors Q2 and Q3, respectively.

4.2 STRUCTURAL INTEGRITY

Postfire examination of motor Q2 nozzle assembly revealed a noticeable separation between the exit cone extension and the glass/epoxy overwrap at the exit cone-to-housing joint (Fig. 5). Further examination at Aerojet revealed that occasional separation is a normal occurrence caused by thermal degradation during cooldown of the overwrap-to-extension cone bond. The extension cone was still intact and engaged in both the aluminum housing and exit cone extension after disassembly. Motor Q3 was tested with no modifications, and separation of the nozzle overwrap again occurred (Fig. 5).

Inspection of both motor cases revealed no "hot spots" or discoloration.

The postfire nozzle throat area of motor Q2 was 6.007 in.² which was a 5.12-percent decrease from the prefire measurement of 6.335 in.²; the postfire throat area of motor Q3 was 6.089 in.² which was a 3.93-percent decrease from the prefire measurement of 6.338 in.². The postfire nozzle exit area of motor Q2 was 339.990 in.² which was an increase of 0.81 percent from the prefire measurement of 337.251 in.²; the nozzle exit area of motor Q3 increased from 337.561 to 340.613 in.² during the firing which was a 0.90-percent increase.

The variation of motor axial forward dome growth relative to the aft skirt attachment ring is shown in Fig. 6 as a function of chamber pressure during the firing. Maximum growth was approximately 0.22 in. for both motors and occurred at the maximum chamber pressure (780 and 670 psia for motors Q2 and Q3, respectively).

Motor case and nozzle temperature variations with time are presented in Fig. 7. The maximum motor case temperature during the motor Q2 firing was approximately 375°F (TC's 16 and 17, Figs. 7d and f) and occurred in the aft section of the motor about 300 sec after motor ignition; maximum motor Q3 case temperature was about 305°F (TC 17, Fig. 7p) and occurred also in the aft section approximately 500 sec after motor ignition. Maximum nozzle temperature during the motor Q2 firing was approximately 625°F (TC-29, Fig. 7g) and occurred near the nozzle exit about 150 sec after ignition; maximum motor Q3 nozzle temperature was about 580°F (TC-29, Fig. 7q) and occurred also near the nozzle exit approximately 125 sec after ignition. All measured temperatures were less than the specification maximum values of 700°F (case) and 800°F (nozzle).

4.3 LATERAL (NONAXIAL) THRUST VECTOR MEASUREMENT

The variation in the nonaxial component of the thrust vector during the motor firings is presented in Fig. 8. The magnitude of the nonaxial vector component ranged from 1 to 7.5 lbf and averaged about 5 lbf for the motor Q2 test, during which the axial force magnitude ranged from 5,000 to 9,000 lbf. The magnitude of the nonaxial vector component ranged from 2 to 19 lbf and averaged about 13 lbf for the motor Q3 firing, during which the axial force magnitude ranged from 4,000 to 7,500 lbf. The corresponding angular location for the maximum thrust vector was 350 and 315 deg for motors Q2 and Q3, respectively.

5.0 SUMMARY OF RESULTS

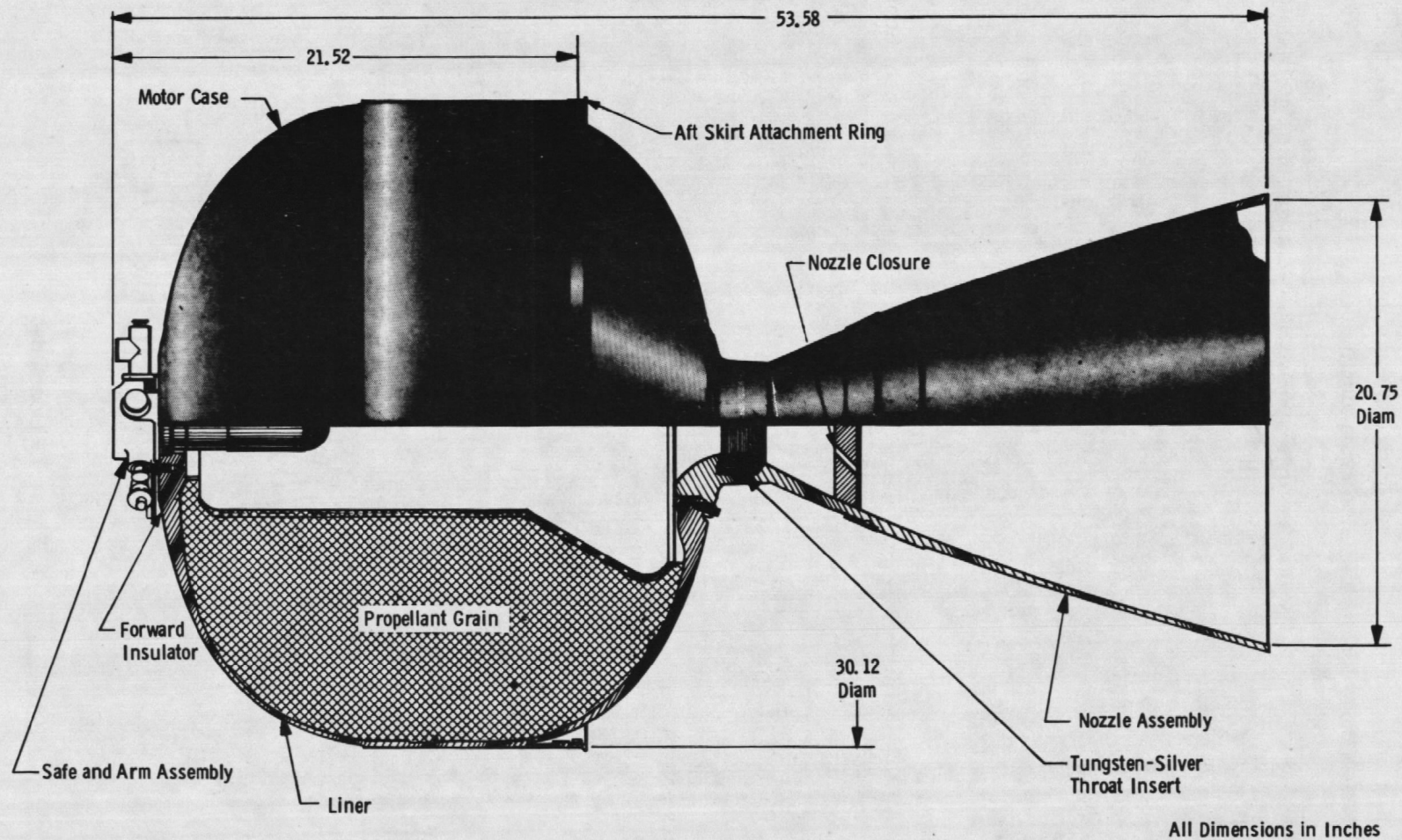
Two Aerojet SVM-6 solid-propellant rocket motors (S/N's Q2 and Q3) were fired at ignition pressure altitudes of 113,000 and 123,000 ft, respectively, as the final part of the SVM-6 qualification test program. The motors were fired while spinning about their axial centerlines at 110 rpm after being preconditioned to a temperature of 110°F (S/N Q2) and 10°F (S/N Q3). The primary objective was to demonstrate compliance with specifications (Ref. 2). The results are summarized below:

1. Ignition time and action time for both motors were well under the specification maximum.
2. Vacuum total impulse, based on total burn time, for both motors was within the specification range of from 208,425 to 211,575 lbf-sec. However, both motors were on the lower end of the specified range (Q2 was 208,433 lbf-sec and Q3 was 208,474 lbf-sec).

3. The maximum measured motor case and nozzle temperatures on both tests were below the specification maximum values.
4. A separation of the nozzle overwrap material occurred during both motor firings. No evidence of thermal damage was apparent.

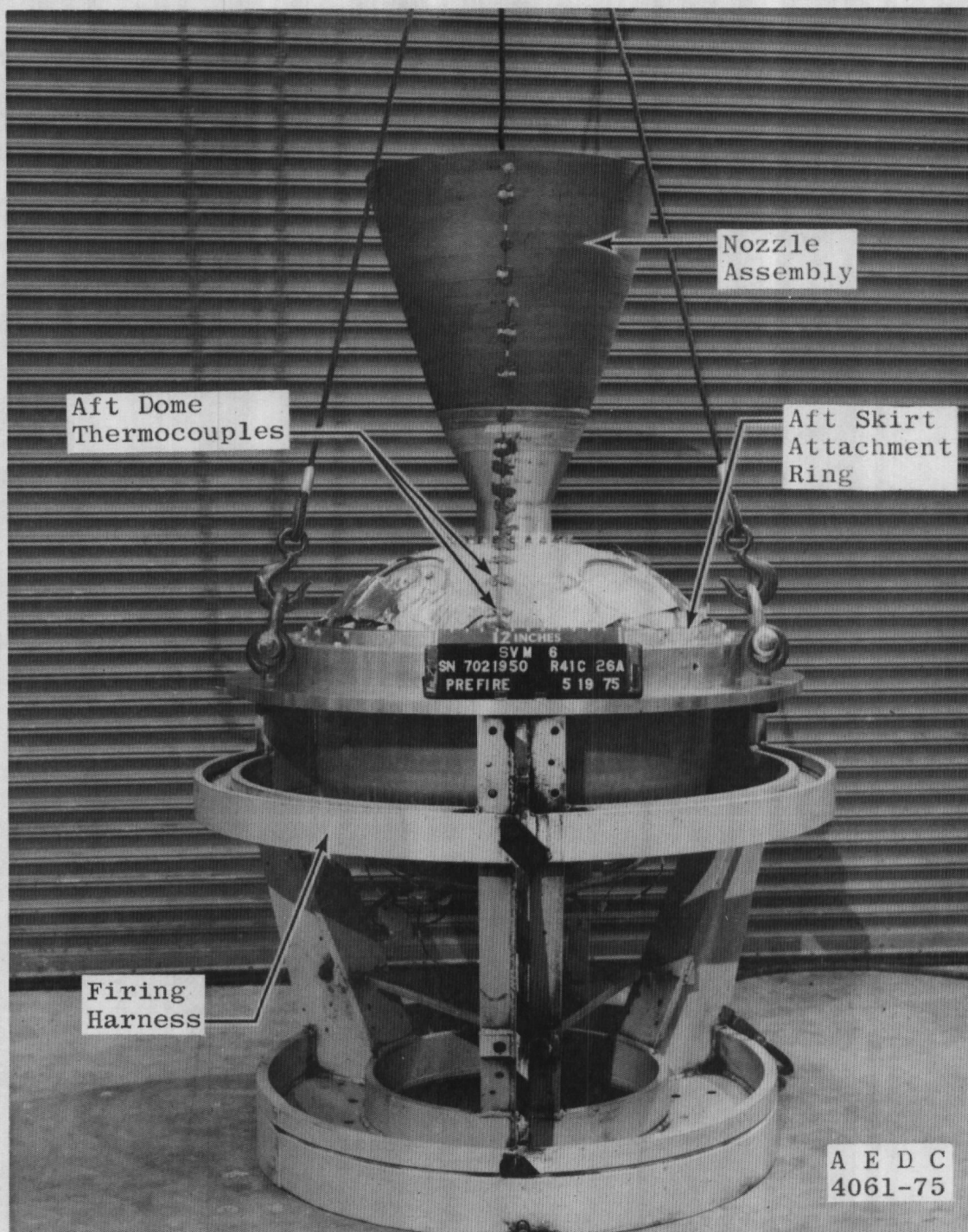
REFERENCES

1. Aerojet Solid Propulsion Co. Report 1059-1B. "Philco-Ford SVM-6 Rocket Motor Qualification Test Plan." June 1974.
2. Philco-Ford Specification AS311332. "Product Specification for Solid Propellant Apogee Kick Motor." May 1973.
3. Nelson, R. "Dynamic Testing of a Philco-Ford/Aerojet SVM-6 NATO III Satcom Apogee Kick Motor (S/N Q-1)." AEDC-TR-74-86 (AD922626L), September 1974.
4. Nelius, M. A. and Brooksbank, R. M. "Altitude Qualification Test of the Philco-Ford/Aerojet SVM-6 NATO III SATCOM Solid-Propellant Rocket Motor (S/N Q-1)." AEDC-TR-74-92 (AD922546L), September 1974.
5. Nelius, M. A. and Harris, J. E. "Measurements of Nonaxial Forces Produced by Solid-Propellant Rocket Motors Using a Spin Technique." AEDC-TR-65-228 (AD74410), November 1965.

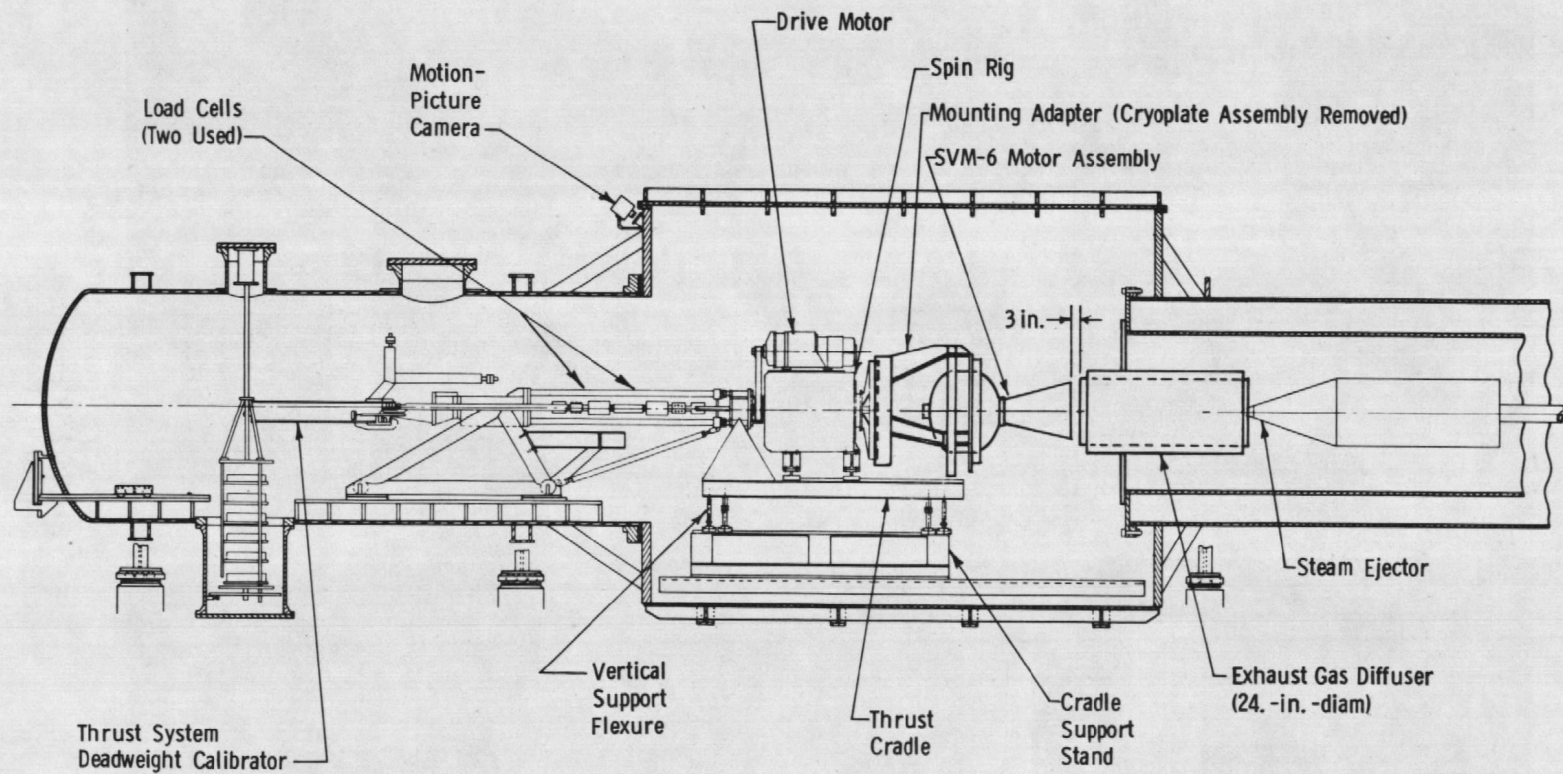


a. Schematic

Figure 1. Aerojet SVM-6 solid-propellant rocket motor.

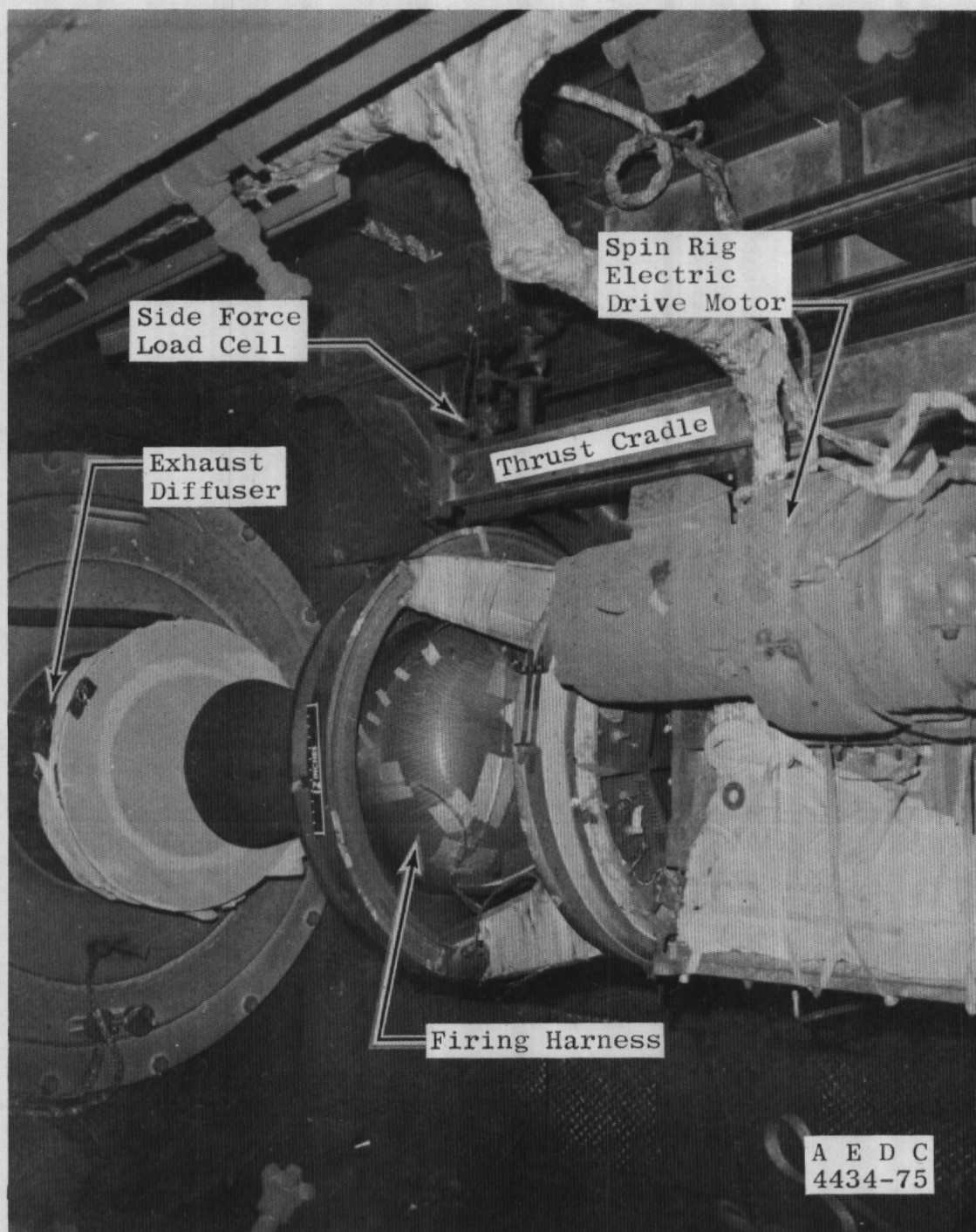


b. Photograph
Figure 1. Concluded.

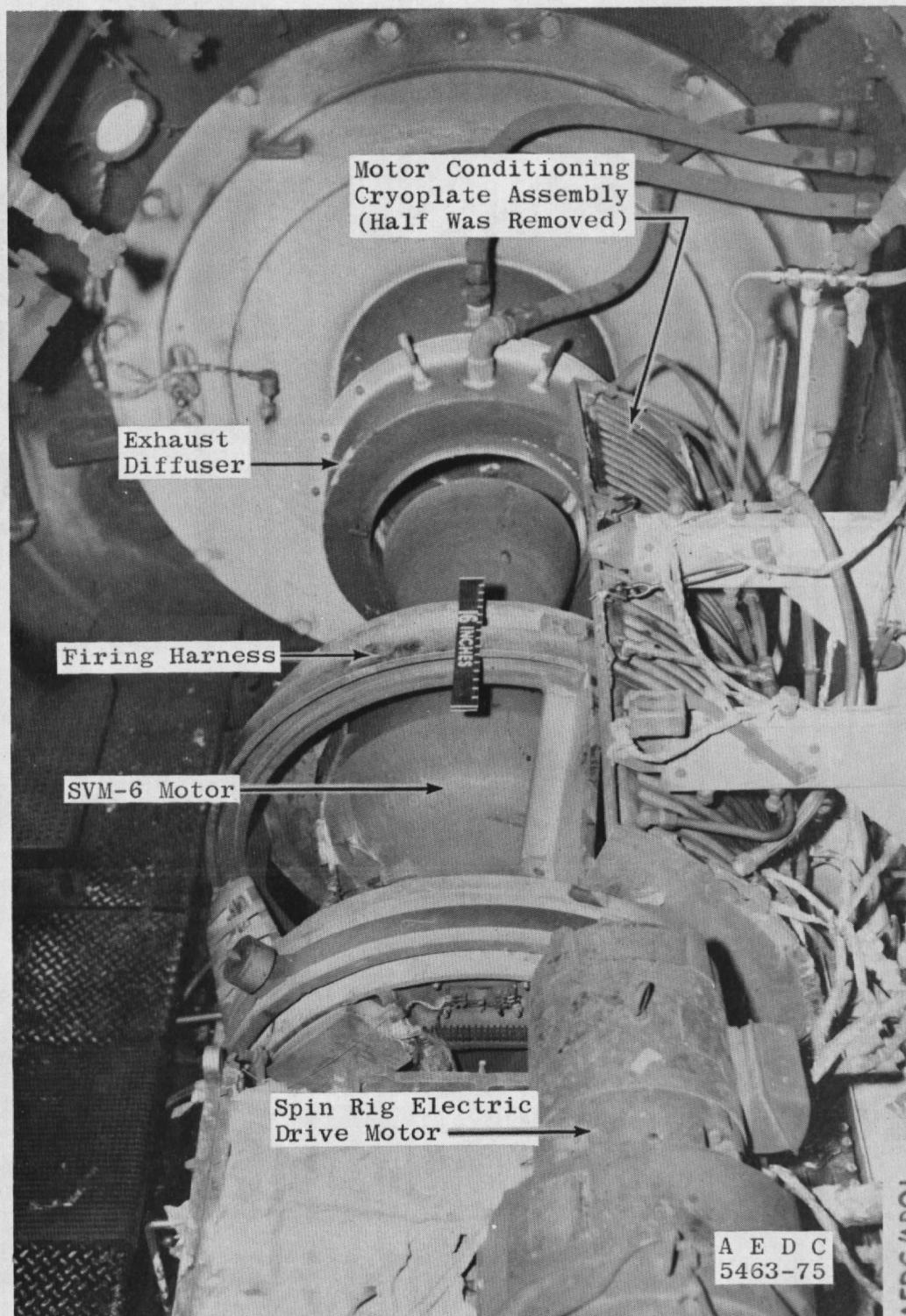


a. Schematic

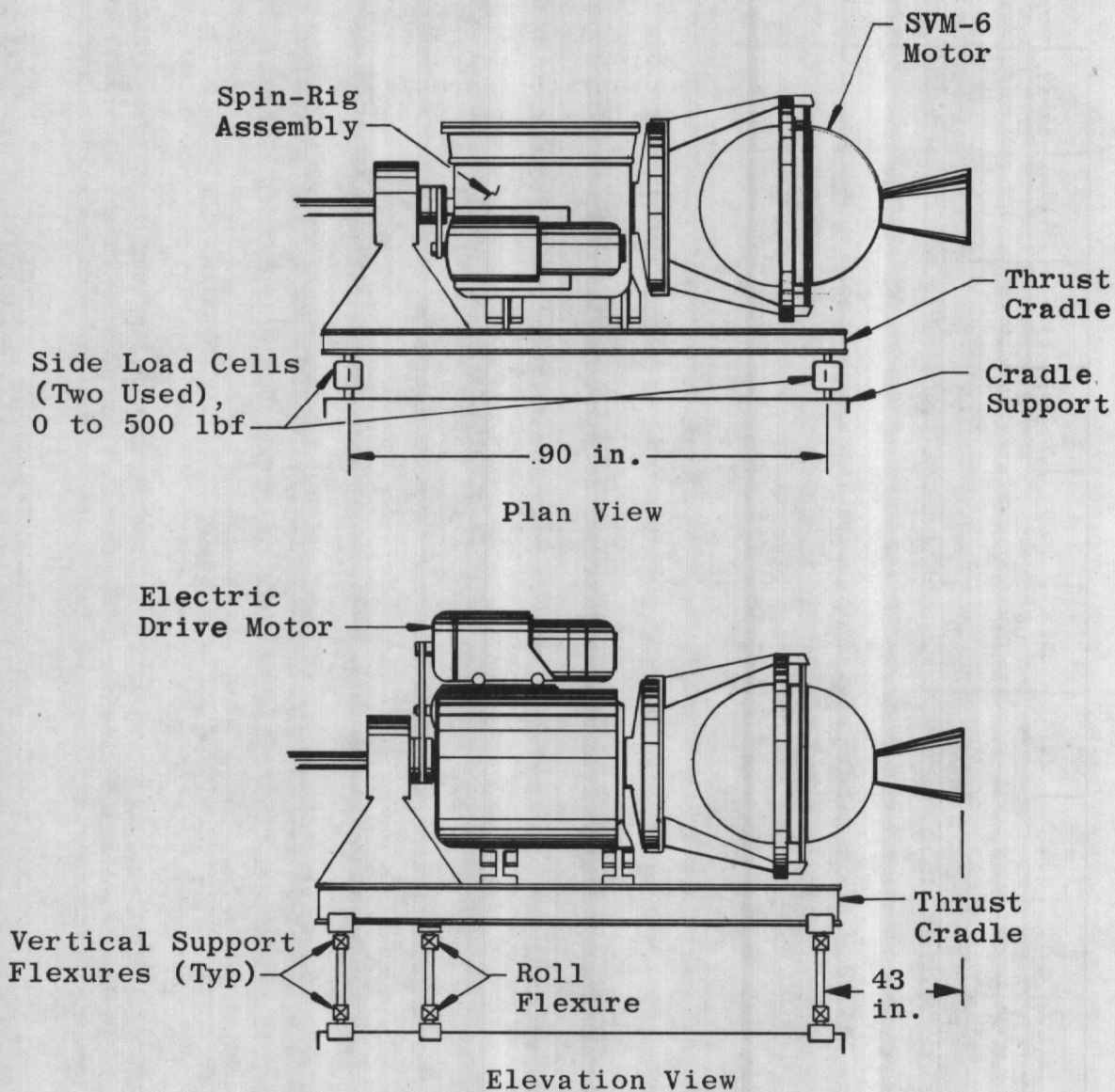
Figure 2. Installation of the Aerojet SVM-6 rocket motor in Propulsion Development Test Cell (T-3).



b. Photograph (motor S/N Q2)
Figure 2. Continued.

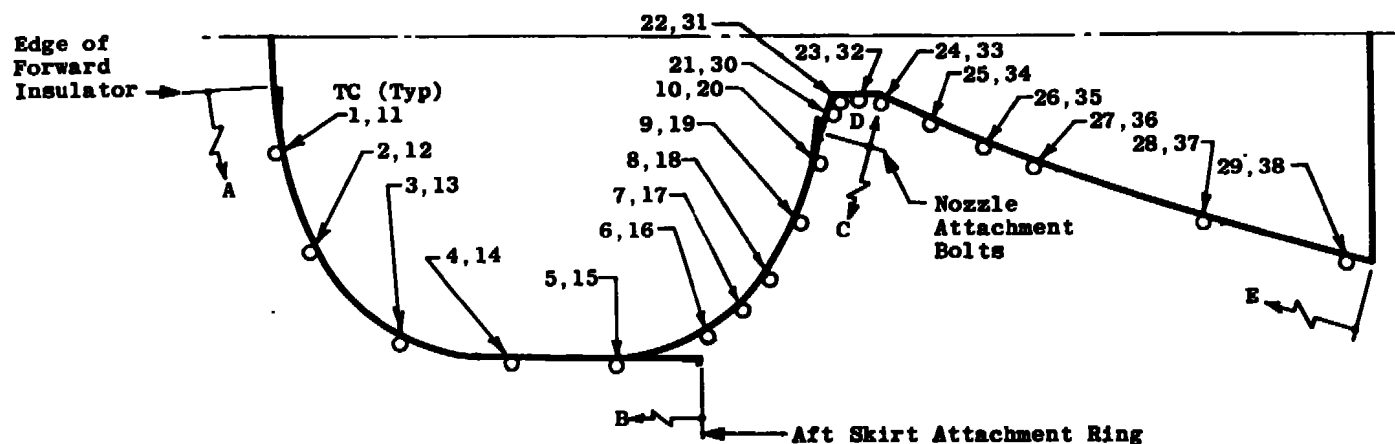


c. Photograph (motor S/N Q3)
Figure 2. Continued.



d. Detail of lateral (nonaxial) force measuring system
Figure 2. Concluded.

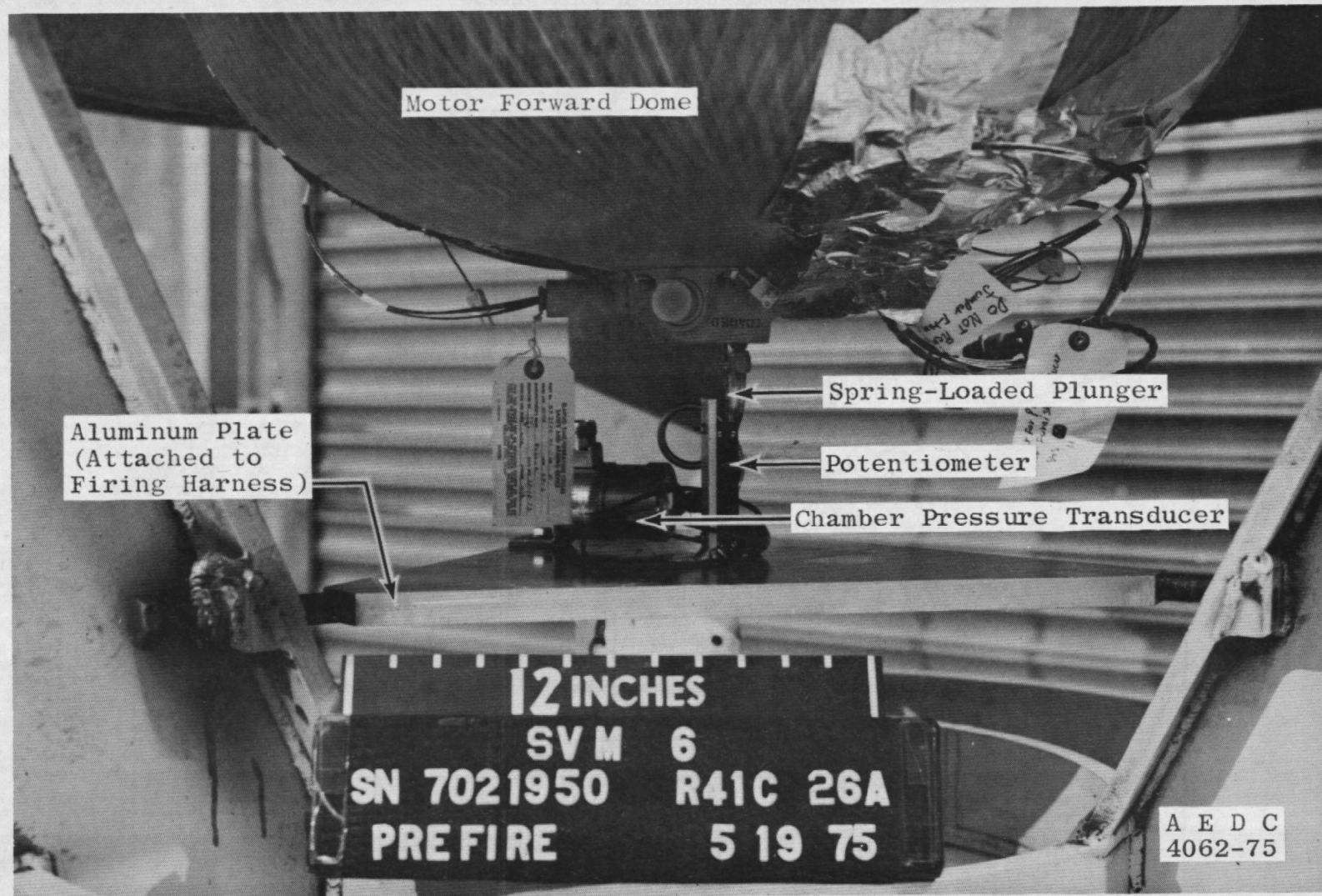
TC No.	1&11	2&12	3&13	4&14	5&15	6&16	7&17	8&18	9&19	10&20
Dim. A	2.6	6.9	12.0							
B				9.0	4.0					
C						11.4	9.9	8.4	5.5	2.5
TC No.	21&30	22&31	23&32	24&33	25&34	26&35	27&36	28&37	29&38	
Dim. D	0.85	1.35								
E			25.40	24.40	22.65	20.90	19.25	9.75	1.0	



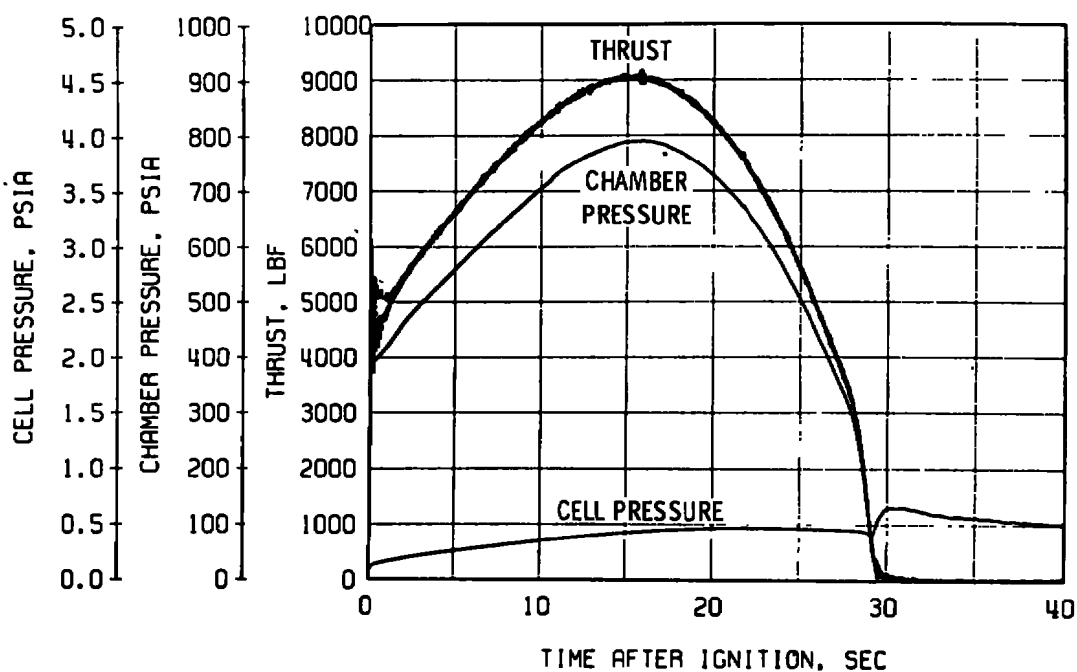
Thermocouples 1 through 10 Located at 90 deg
 Thermocouples 11 through 20 Located at 270 deg
 Thermocouples 21 through 29 Located at 0 deg
 Thermocouples 30 through 38 Located at 180 deg

a. Thermocouples

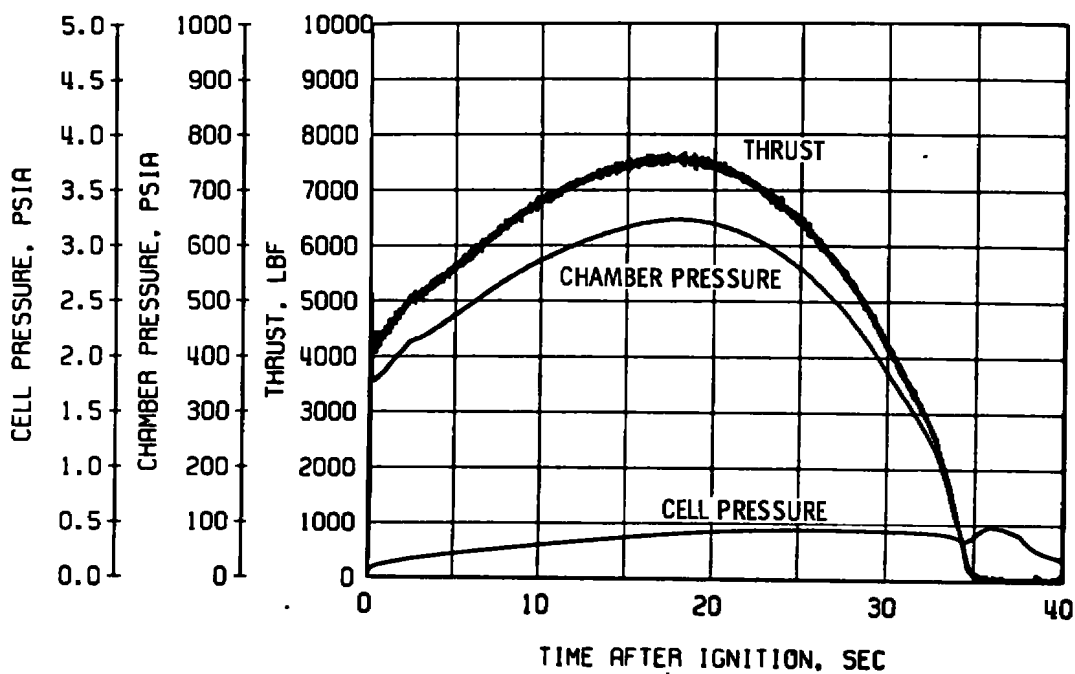
Figure 3. Instrumentation locations.



b. Forward dome growth potentiometer
Figure 3. Concluded.

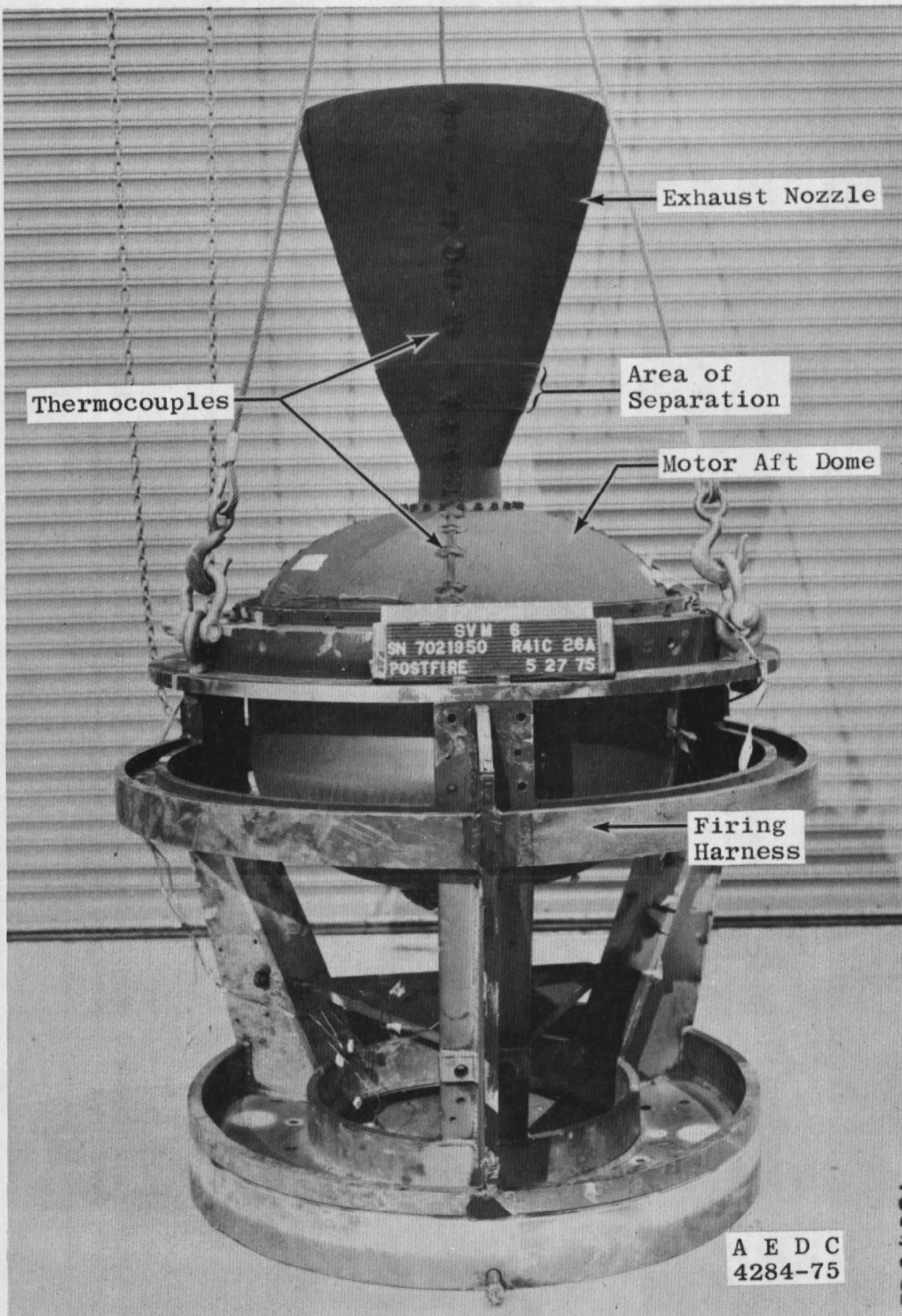


a. Motor S/N Q2



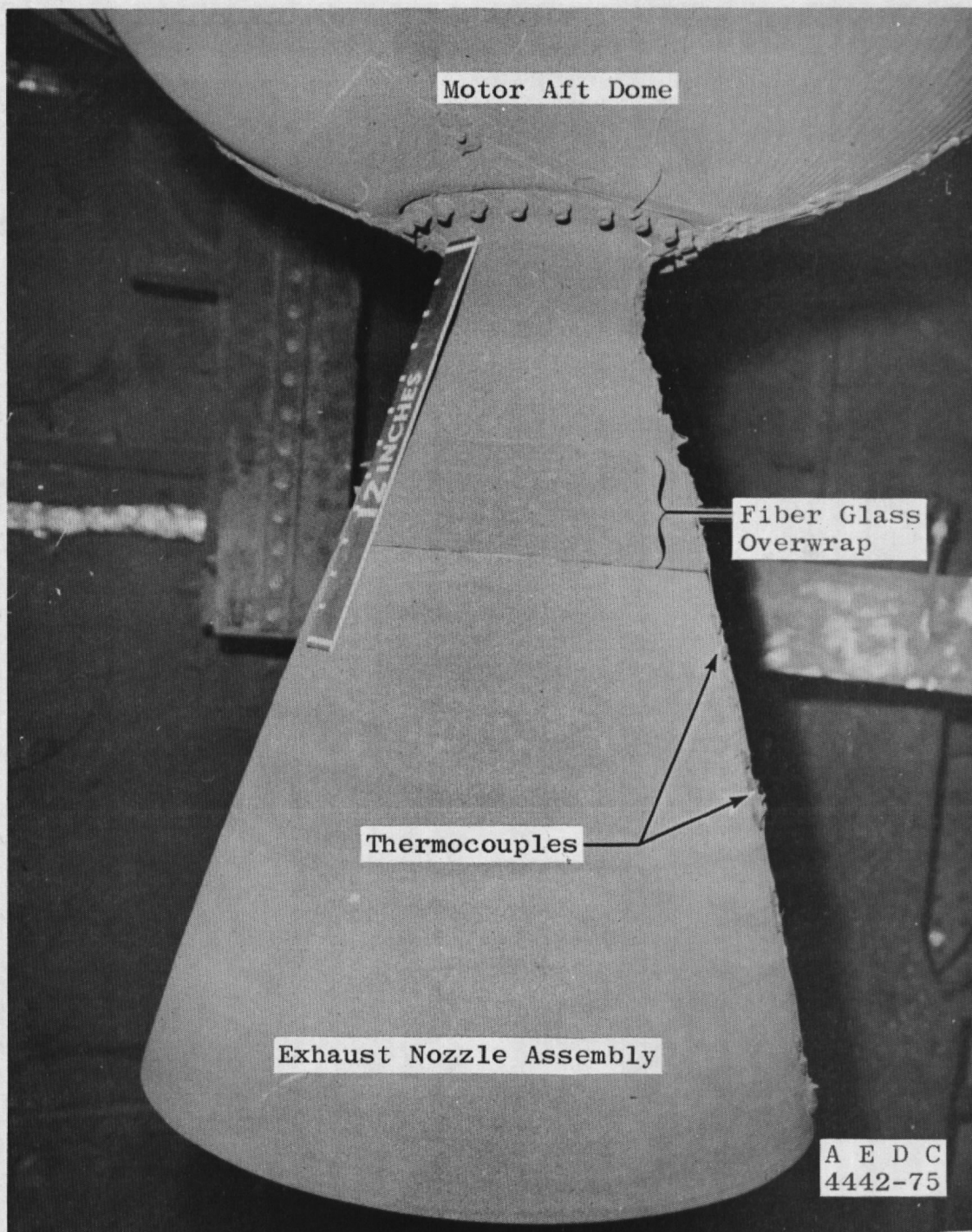
b. Motor S/N Q3

Figure 4. Variation in thrust, chamber pressure, and cell pressure during firing.

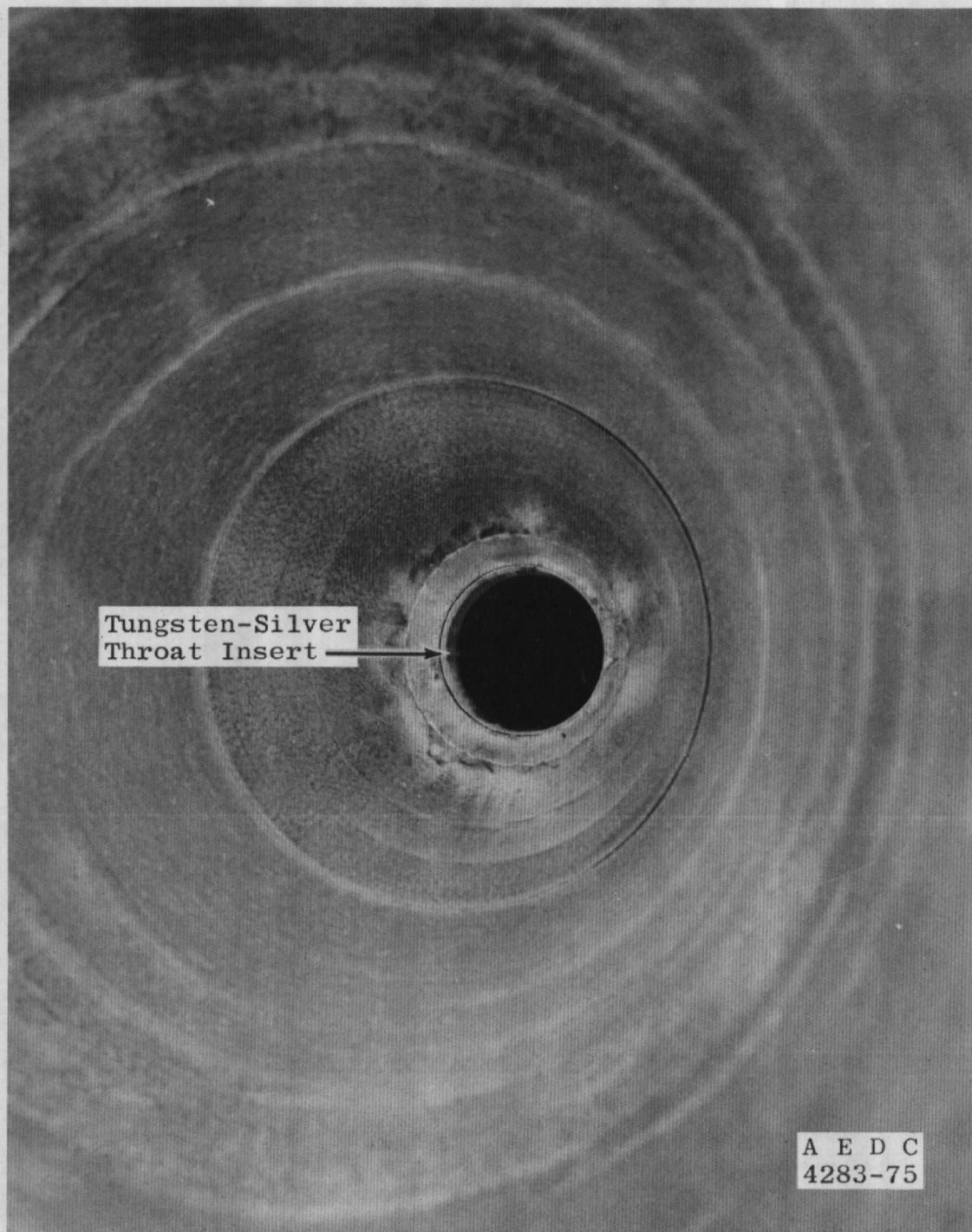


a. Motor Q2

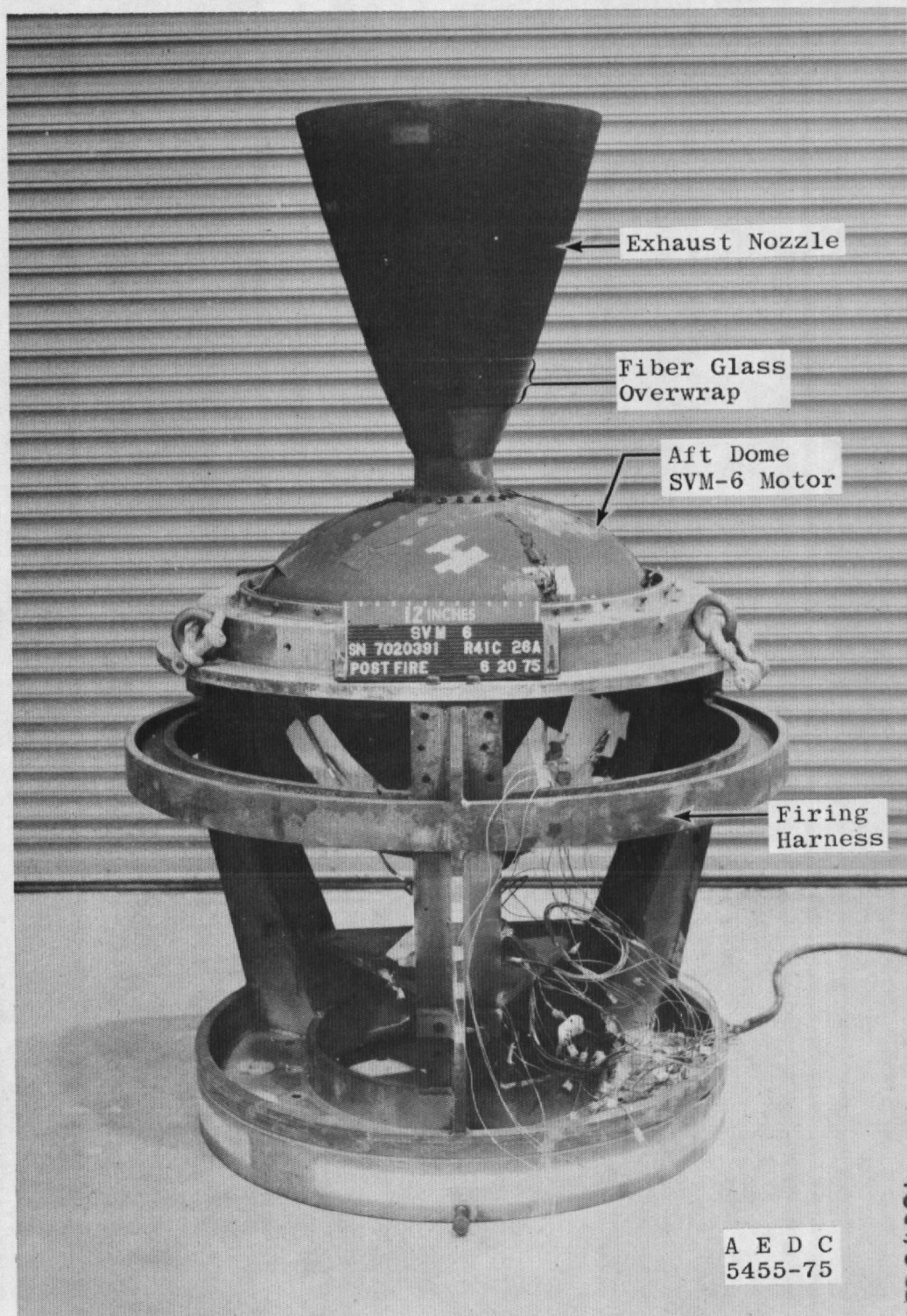
Figure 5. Postfire photographs of the motor assembly.



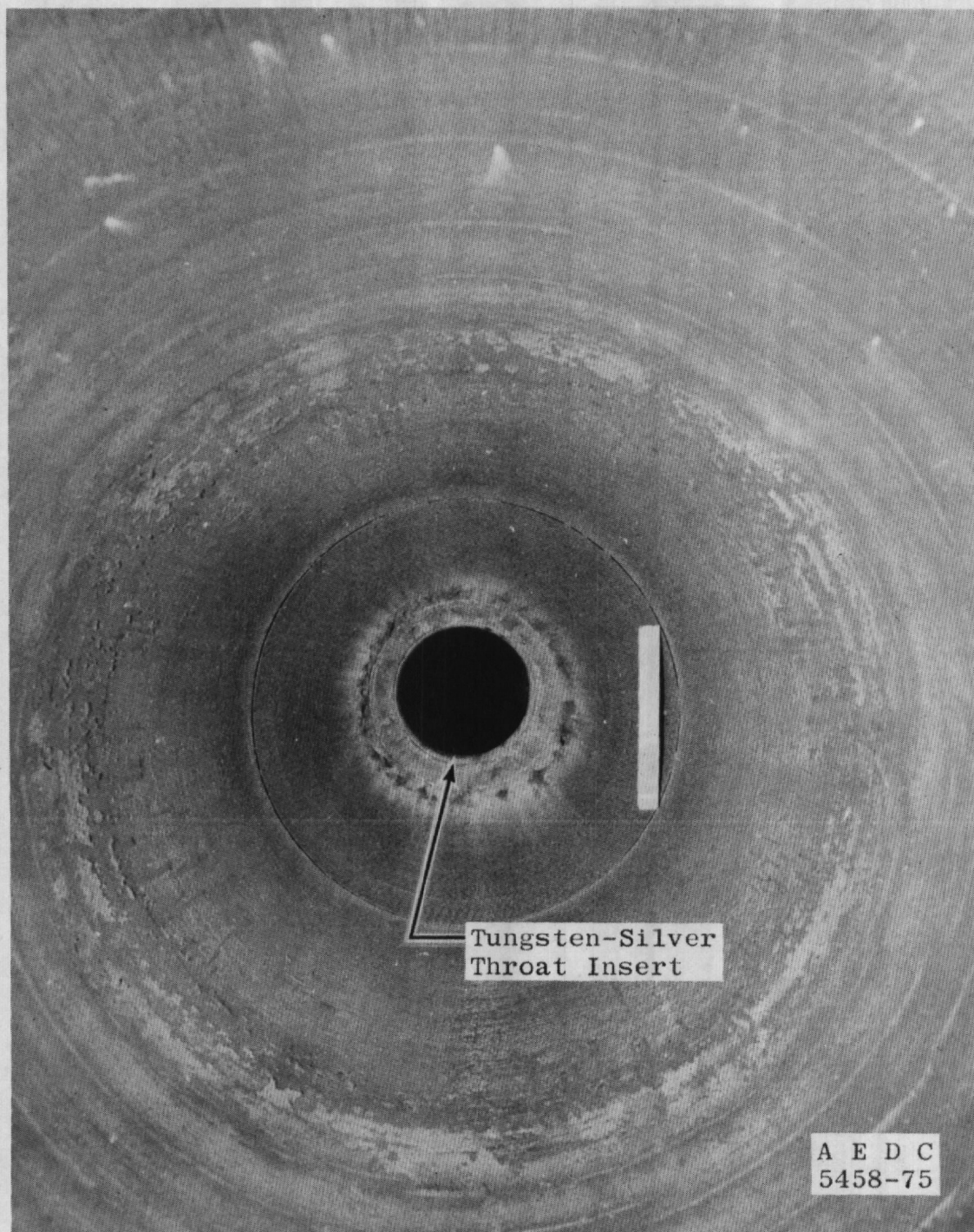
b. Nozzle assembly (motor Q2)
Figure 5. Continued.



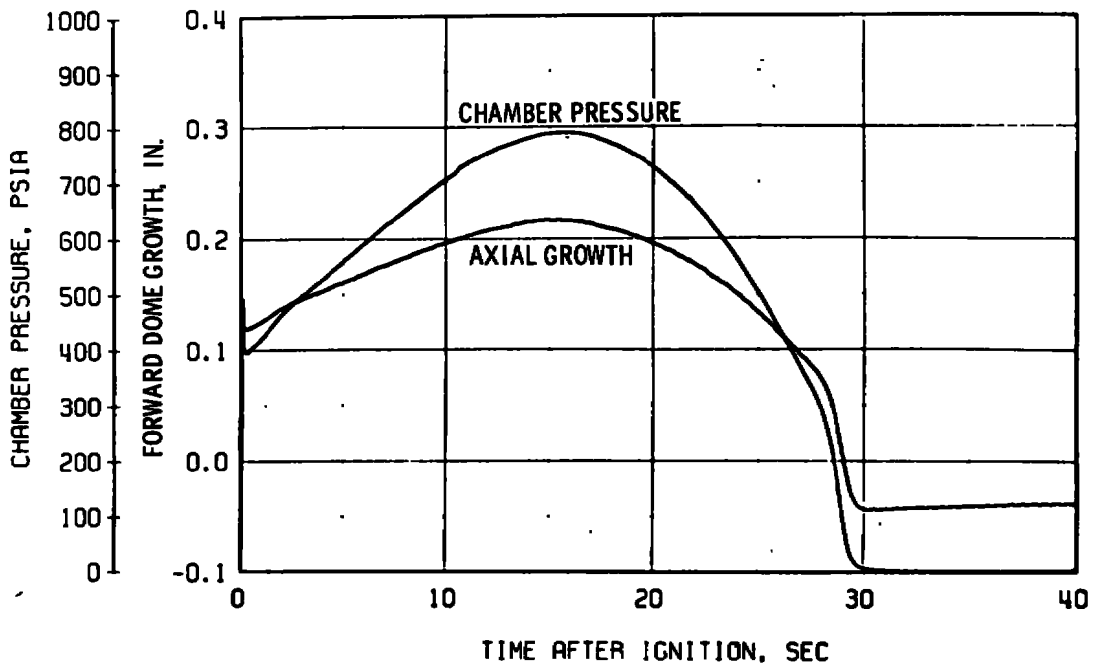
c. Nozzle throat (motor Q2)
Figure 5. Continued.



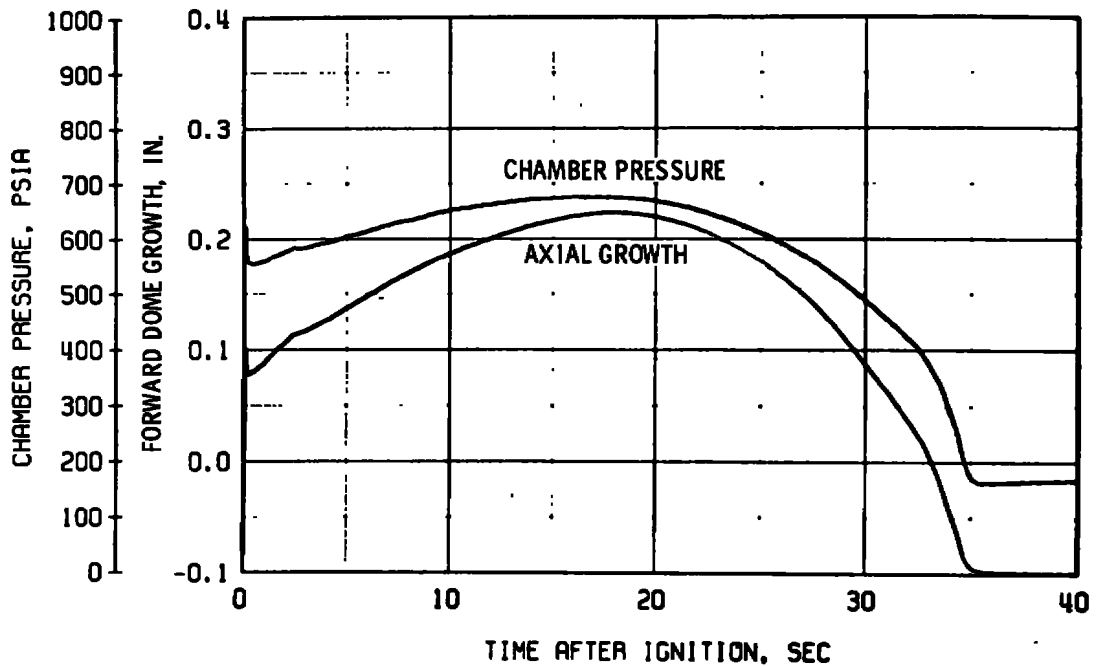
d. Motor Q3
Figure 5. Continued.



e. Nozzle throat (motor Q3)
Figure 5. Concluded.

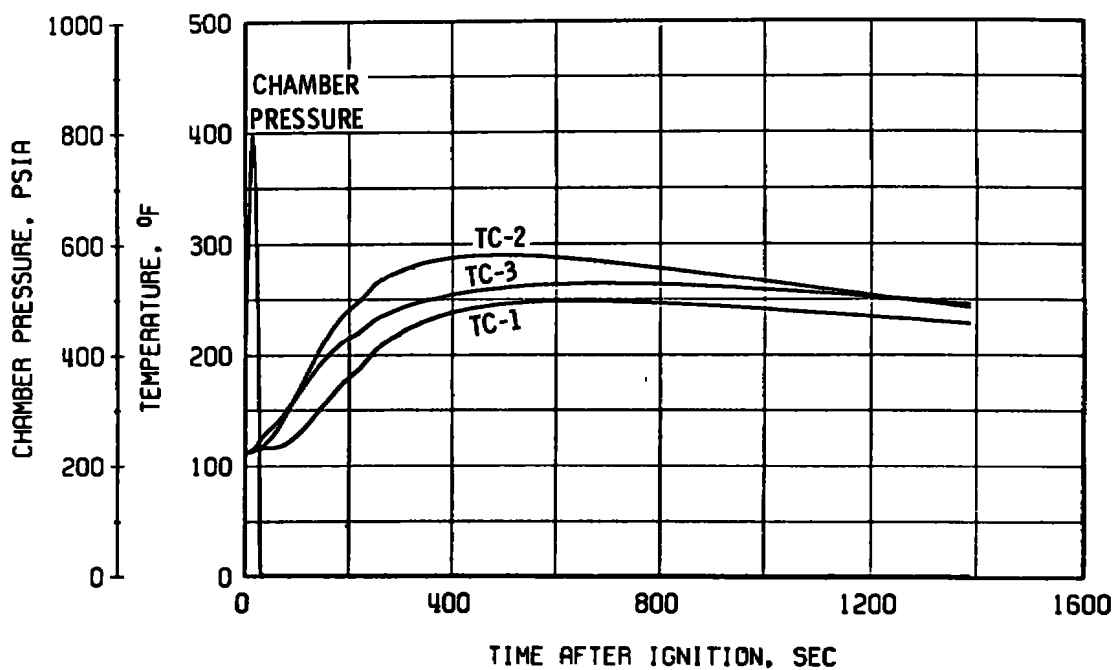


a. Motor Q2

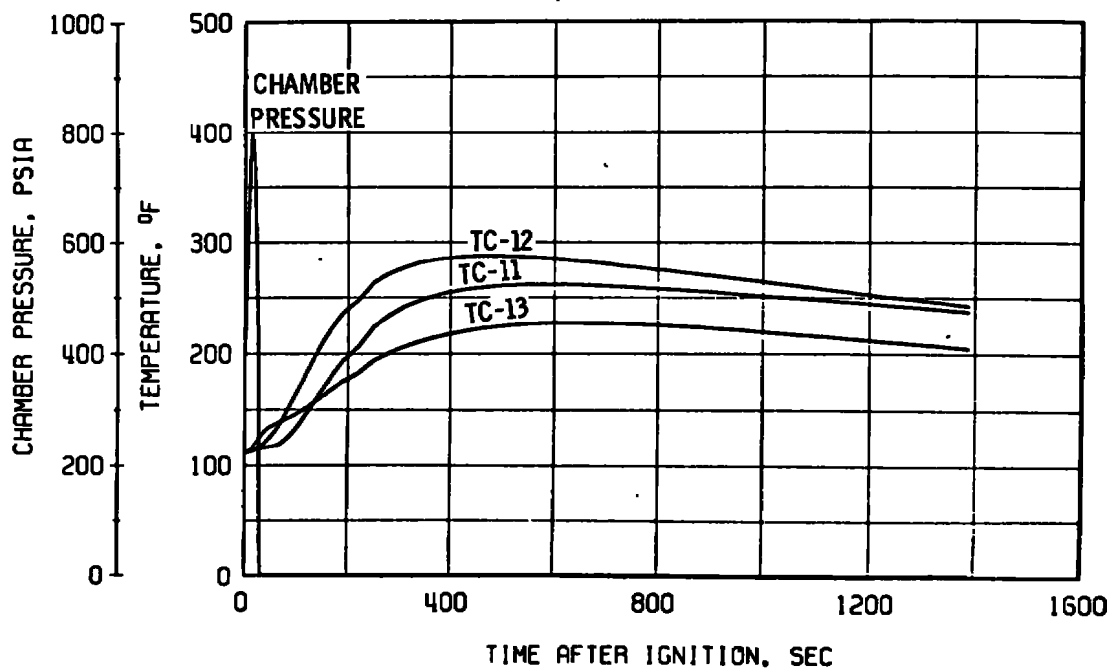


b. Motor Q3

Figure 6. Forward dome axial growth relative to aft skirt attachment ring.

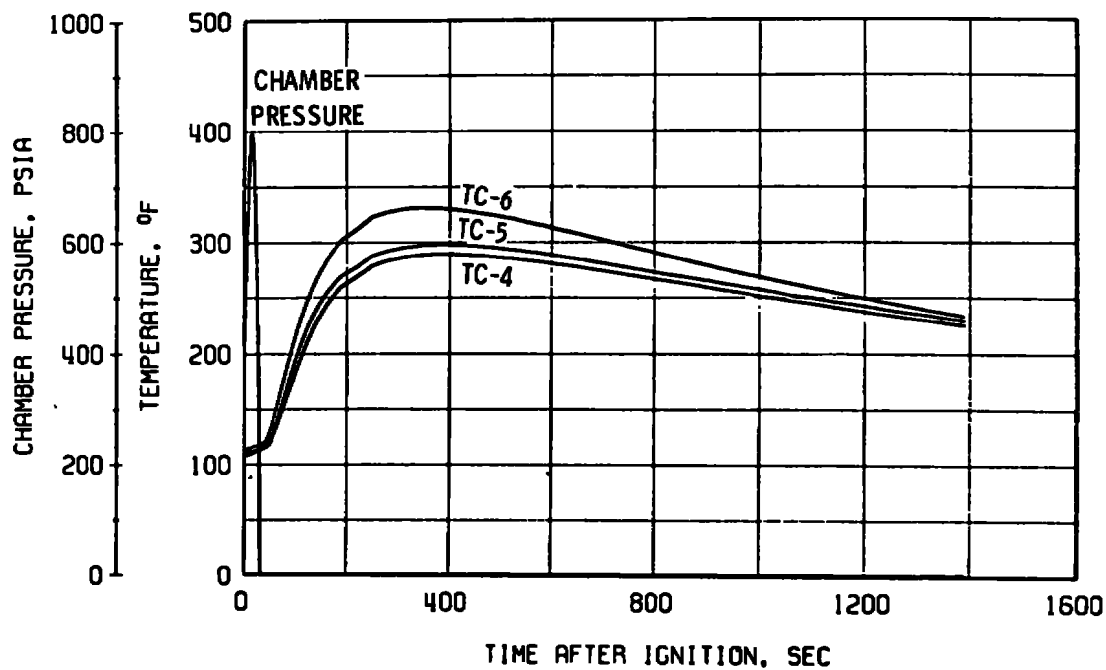


a. Forward dome (Q2)

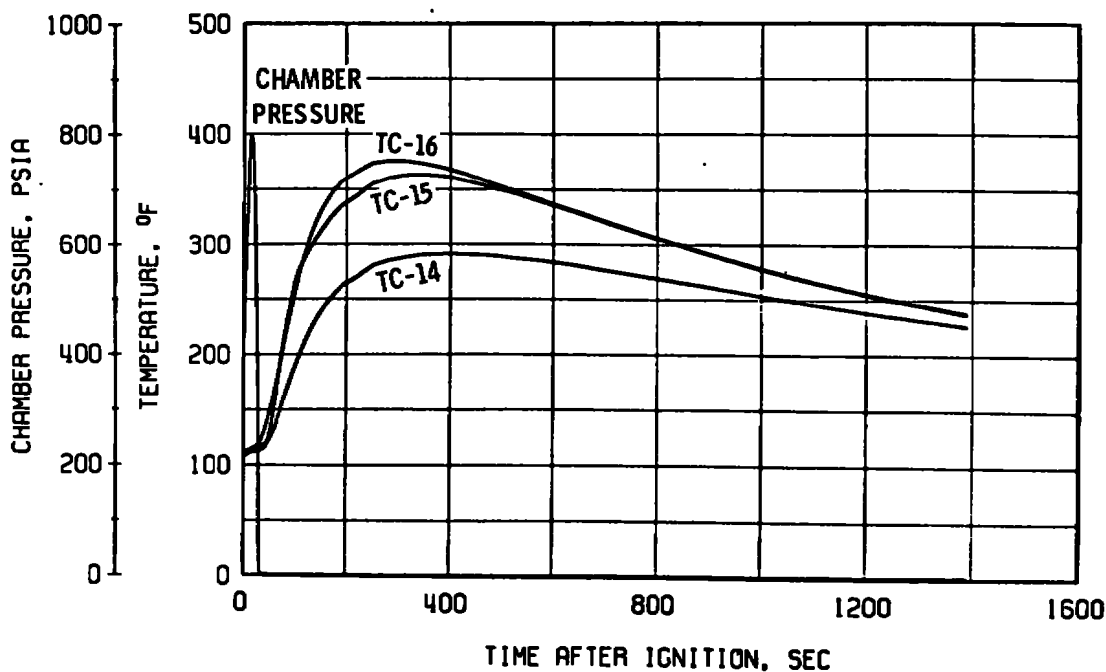


b. Forward dome (Q2)

Figure 7. Motor temperature variation with time.

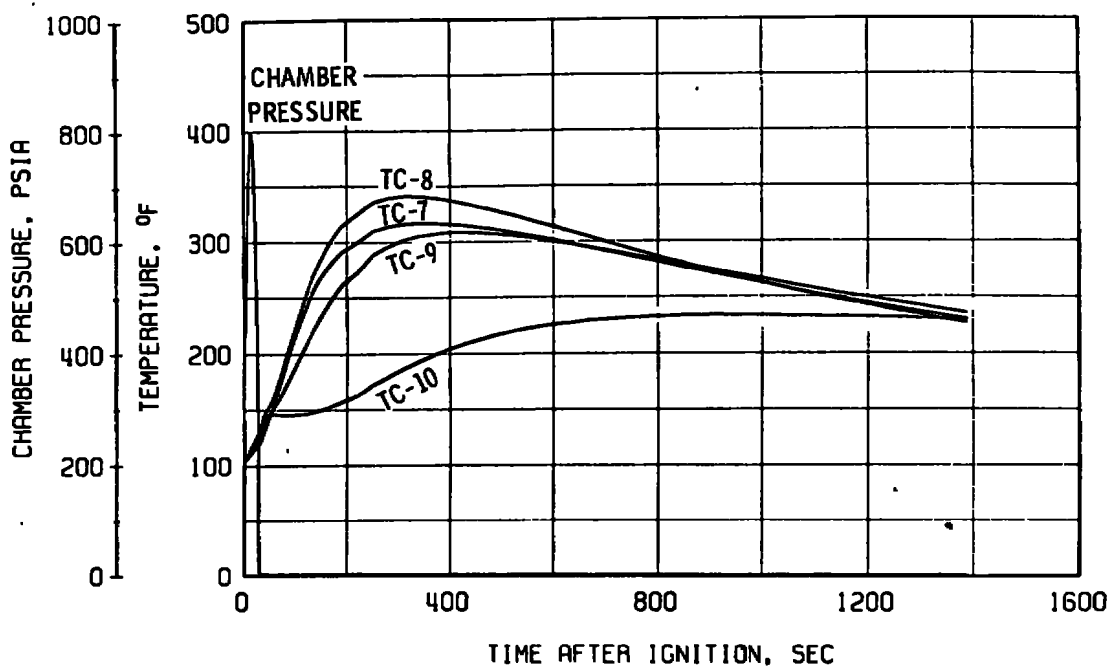


c. Case (Q2)

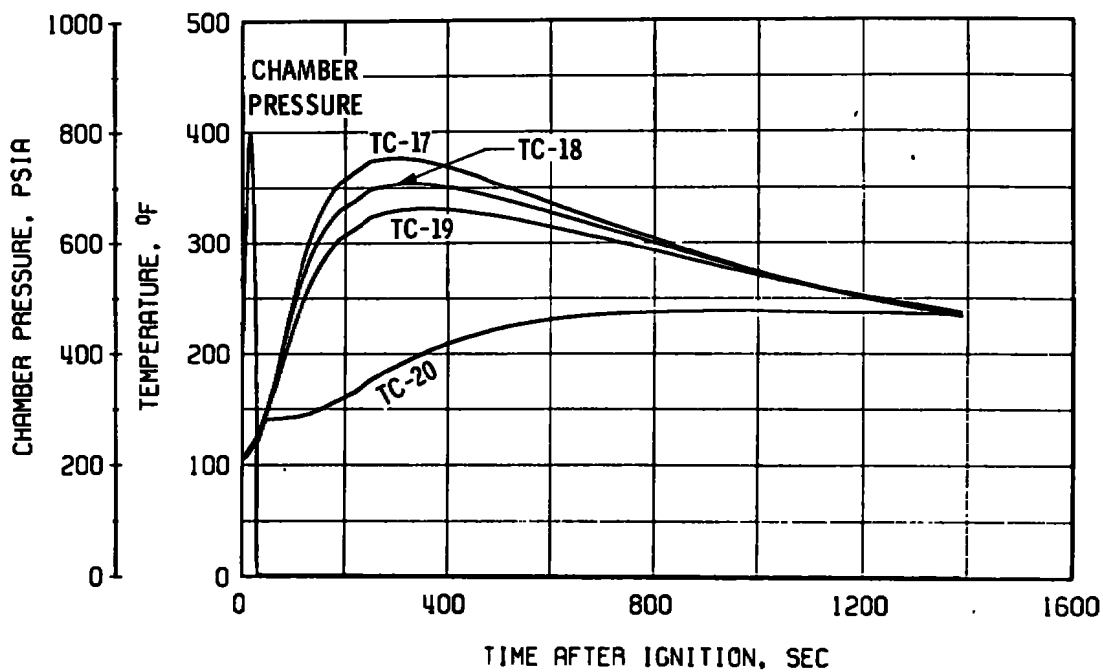


d. Case (Q2)

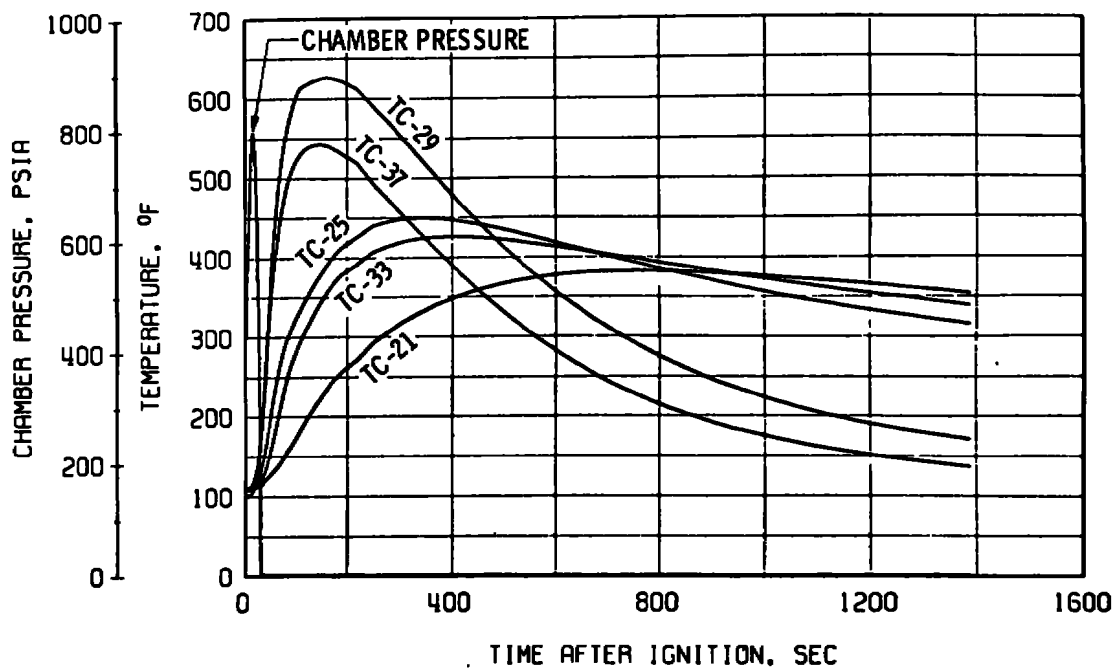
Figure 7. Continued.



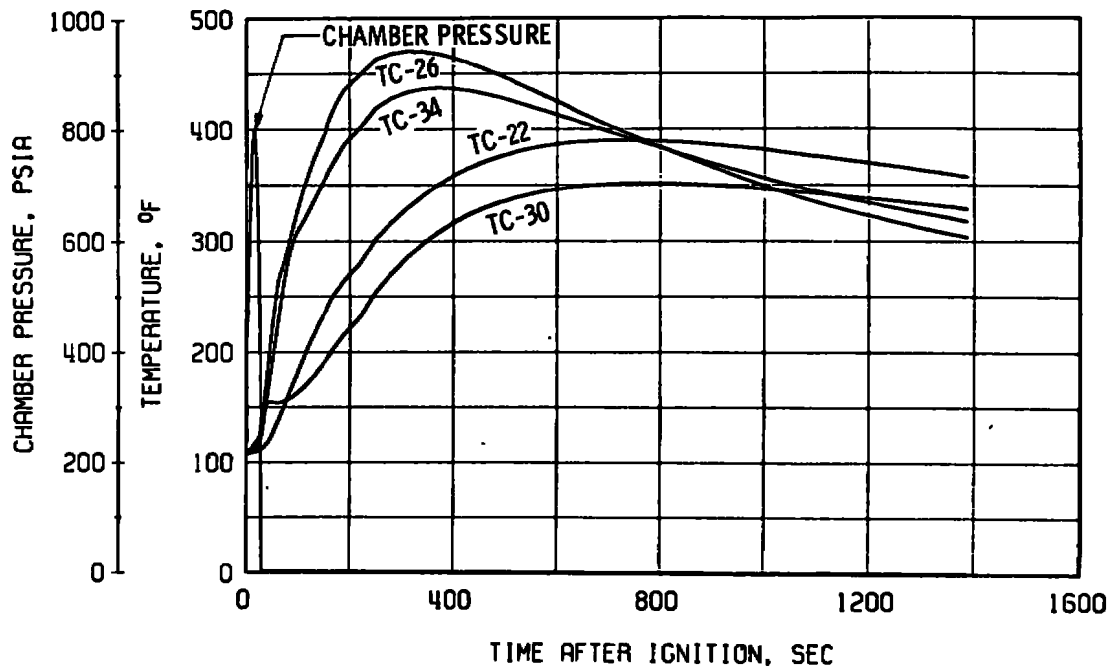
e. Aft dome (Q2)



f. Aft dome (Q2)
Figure 7. Continued.

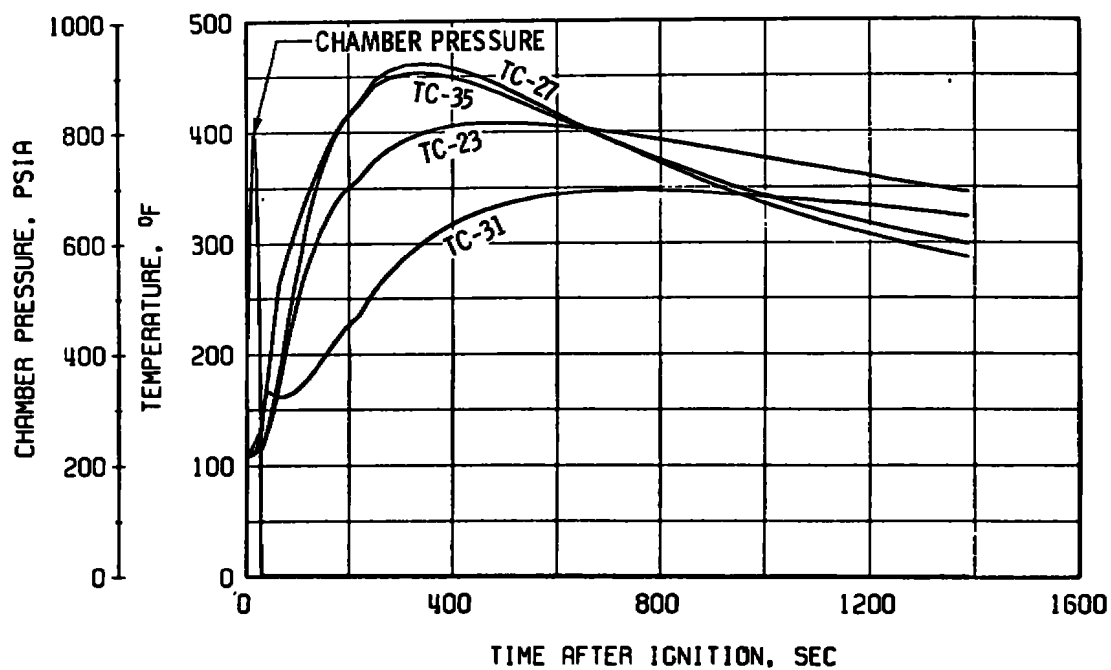


g. Exhaust nozzle (Q2)

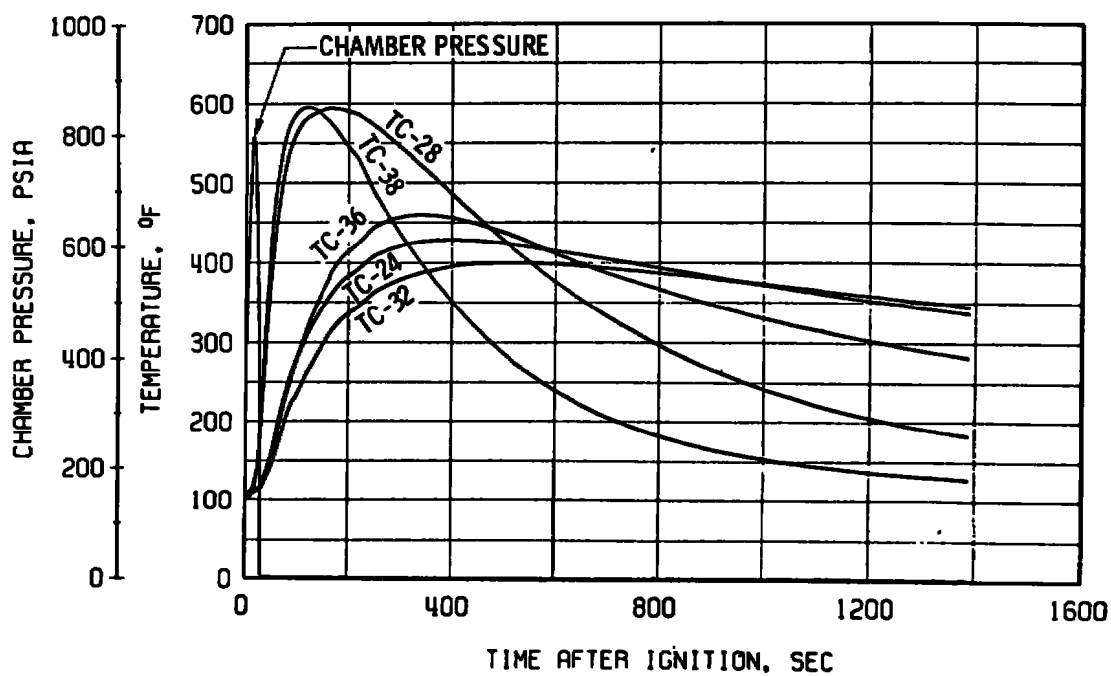


h. Exhaust nozzle (Q2)

Figure 7. Continued.

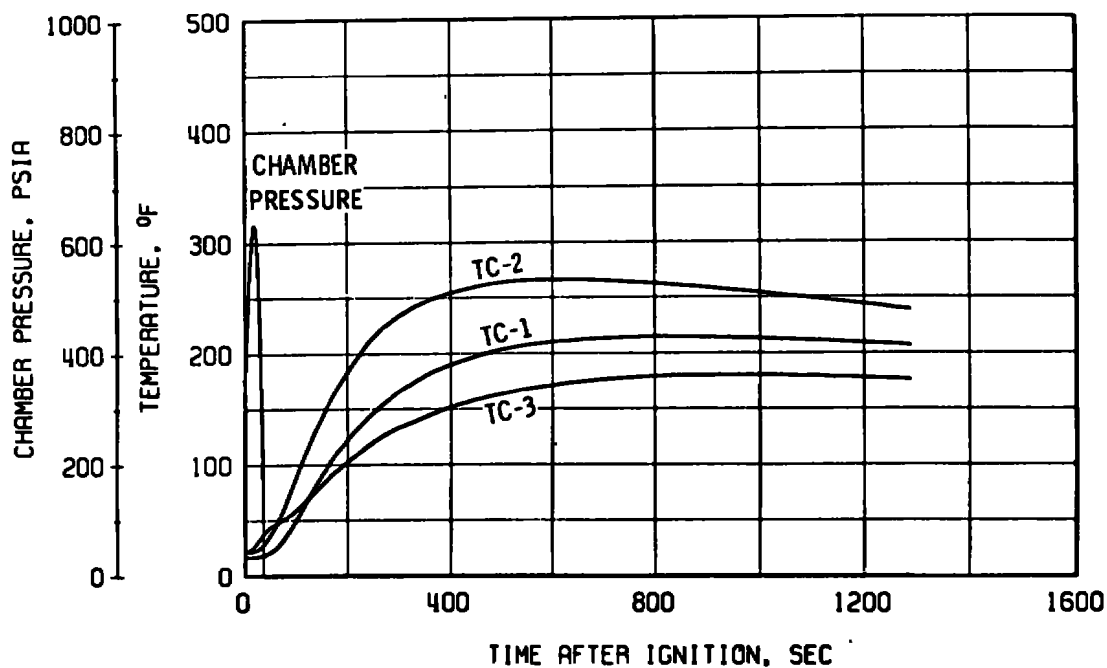


i. Exhaust nozzle (Q2)

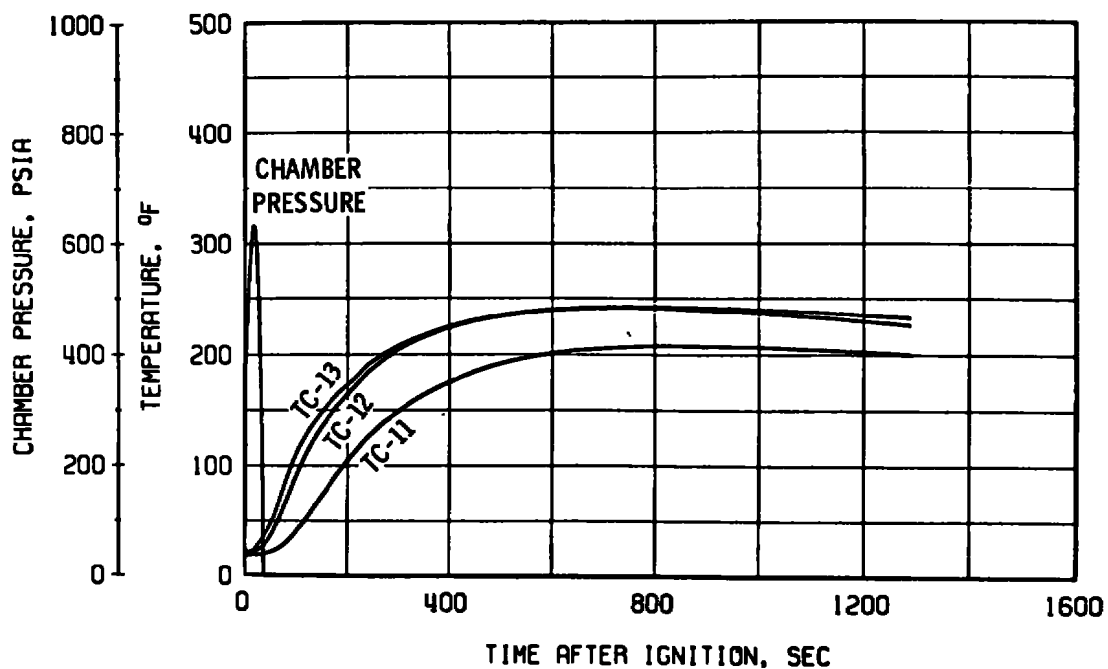


j. Exhaust nozzle (Q2)

Figure 7. Continued.

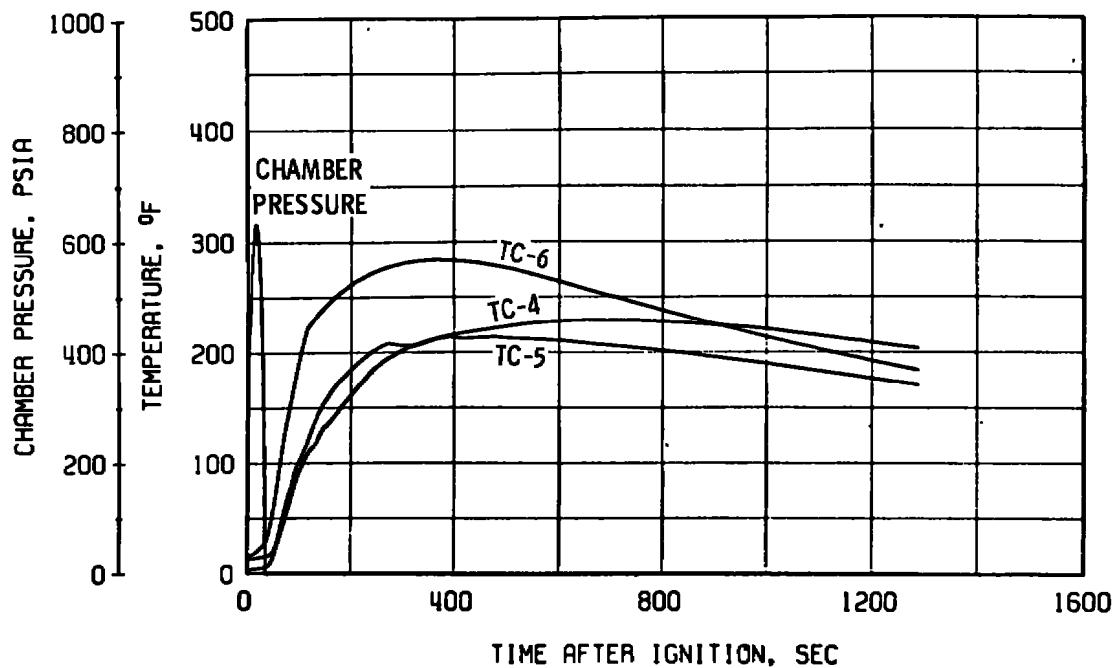


k. Forward dome (Q3)

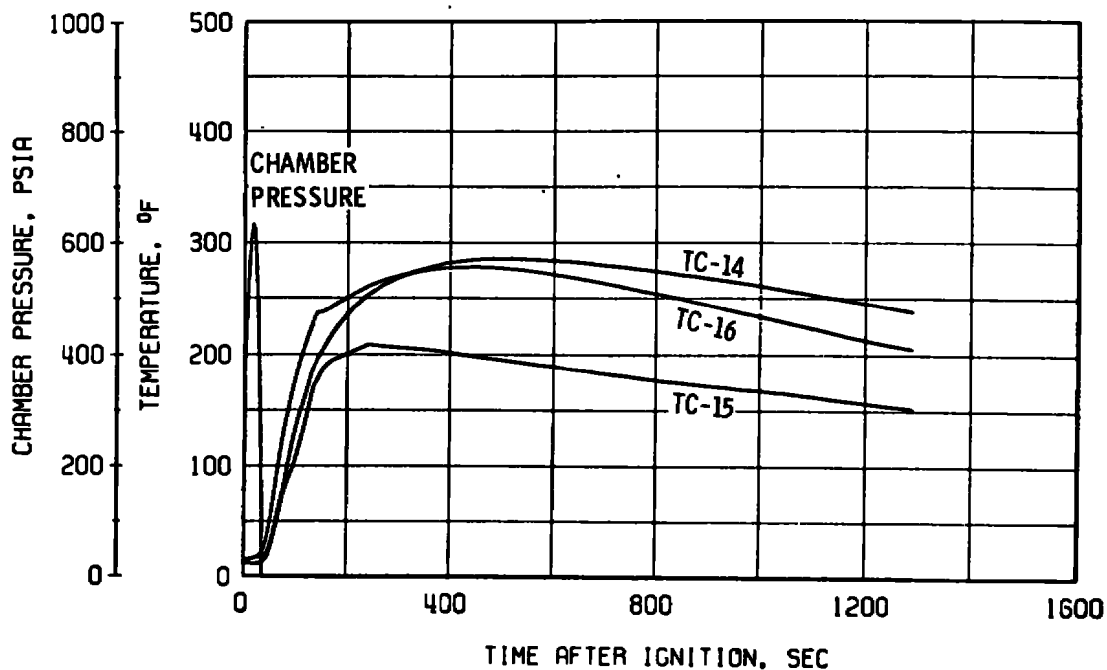


l. Forward dome (Q3)

Figure 7. Continued.

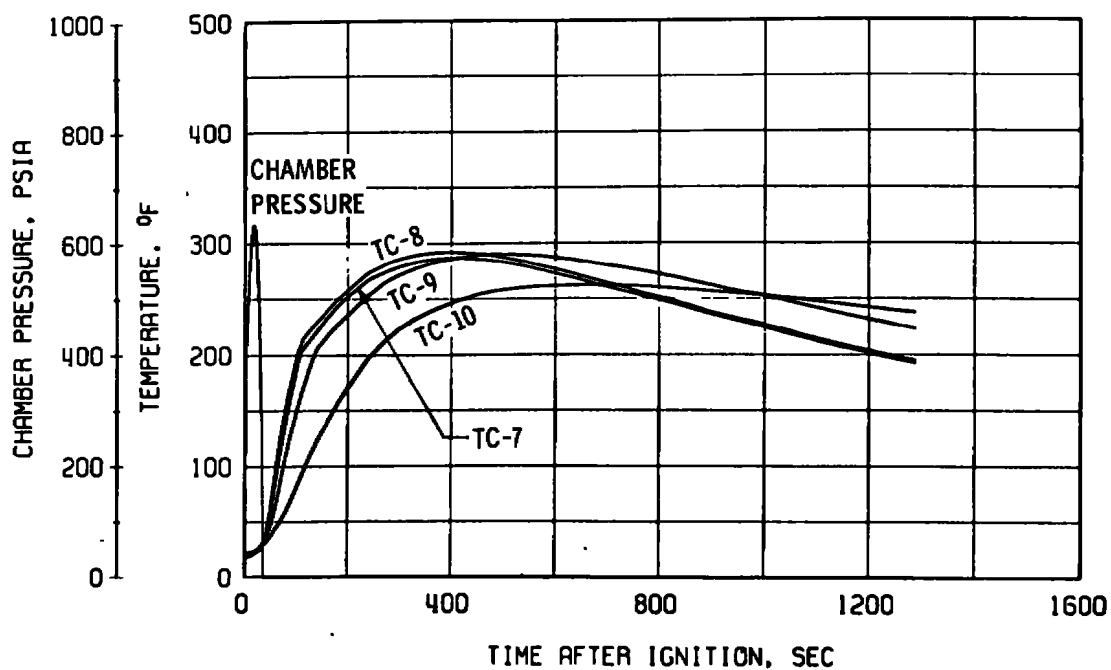


m. Case (Q3)

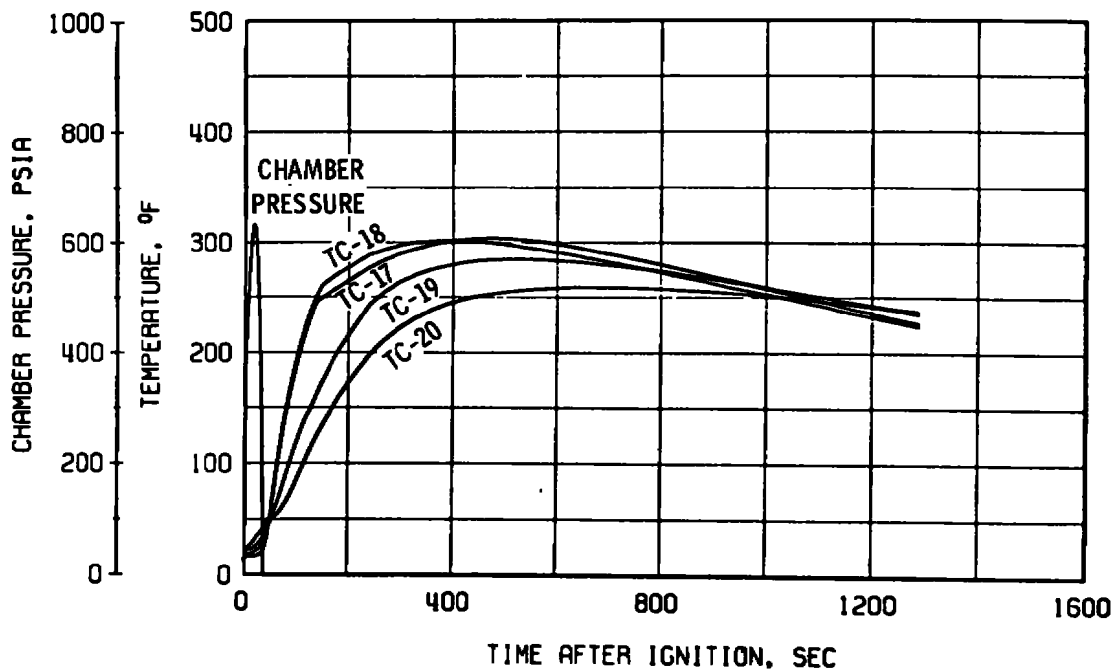


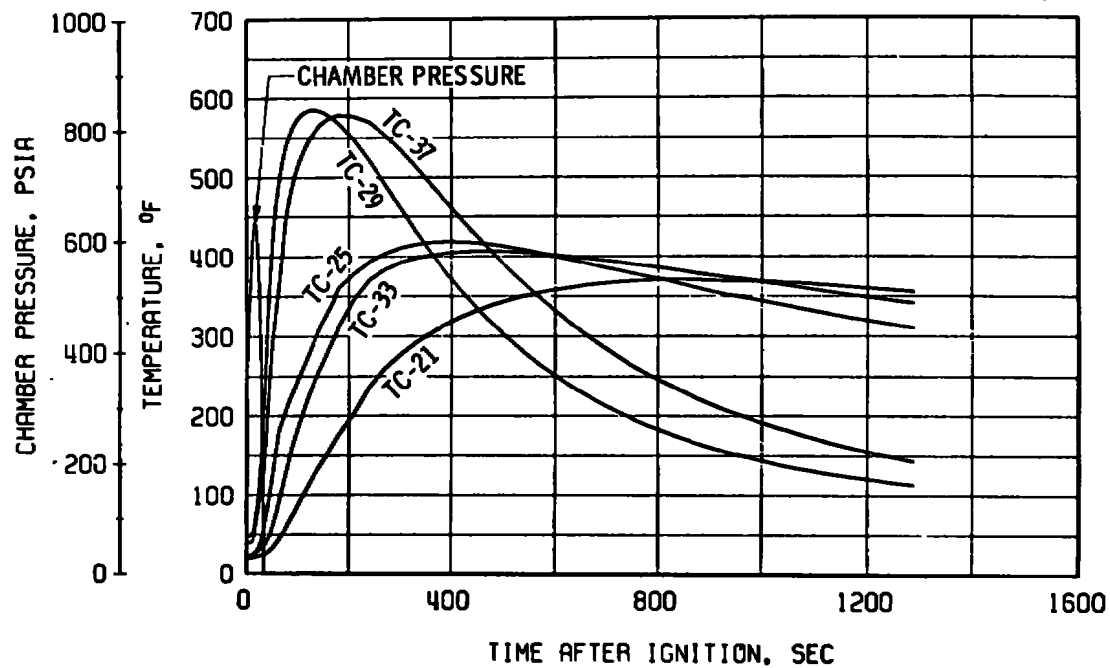
n. Case (Q3)

Figure 7. Continued.

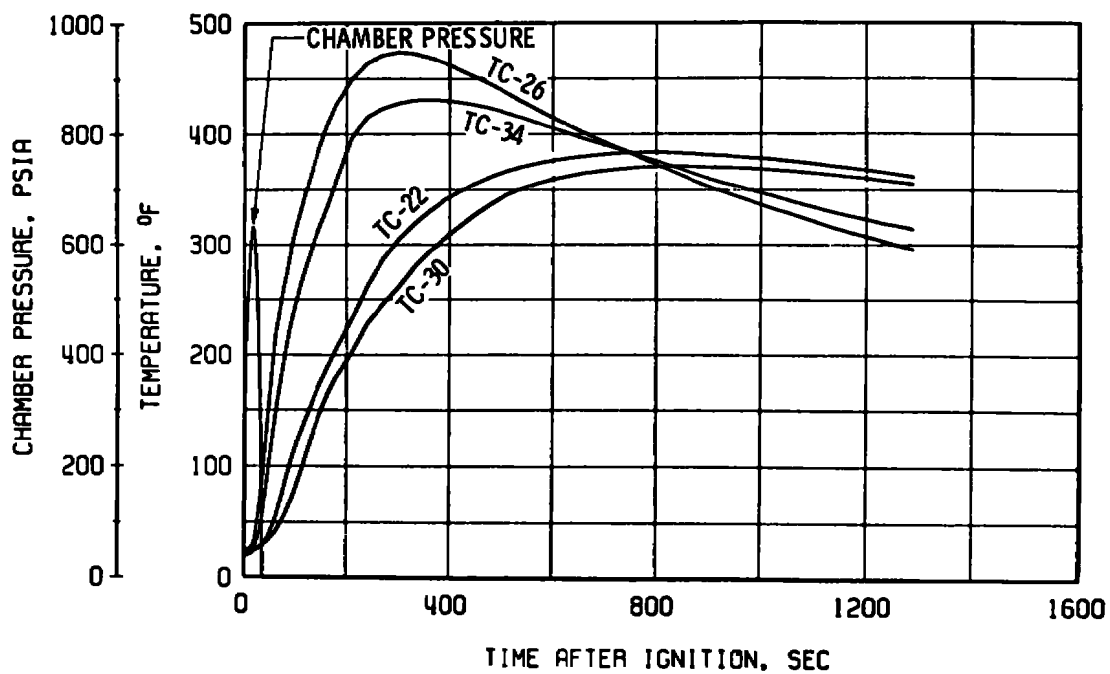


o. Aft dome (Q3)

p. Aft dome (Q3)
Figure 7. Continued.

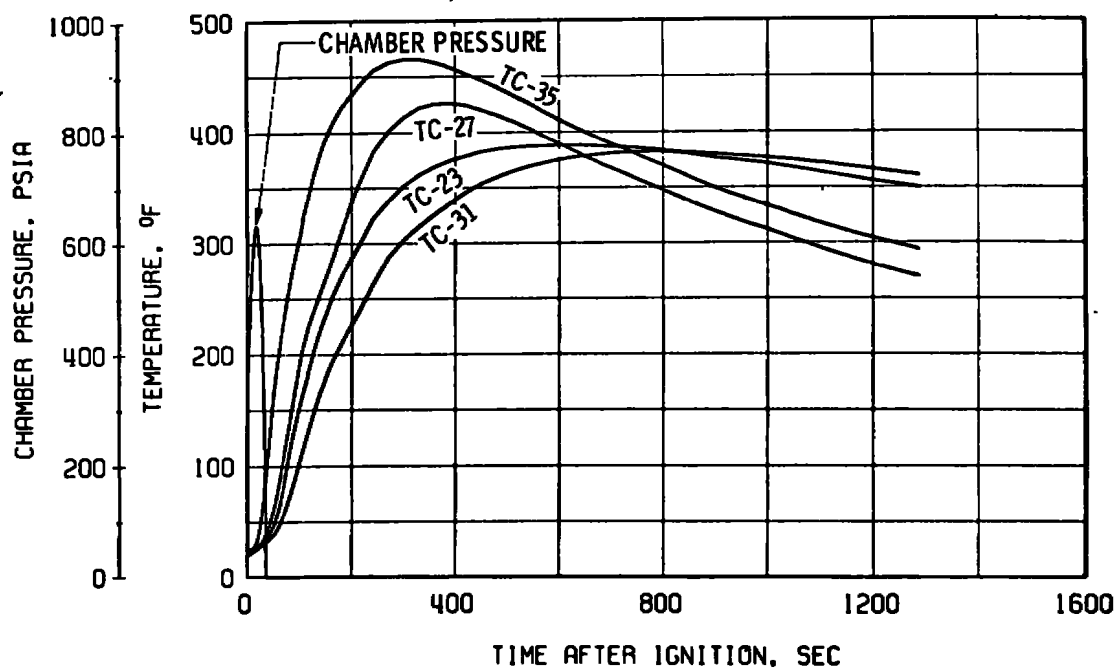


q. Exhaust nozzle (Q3)

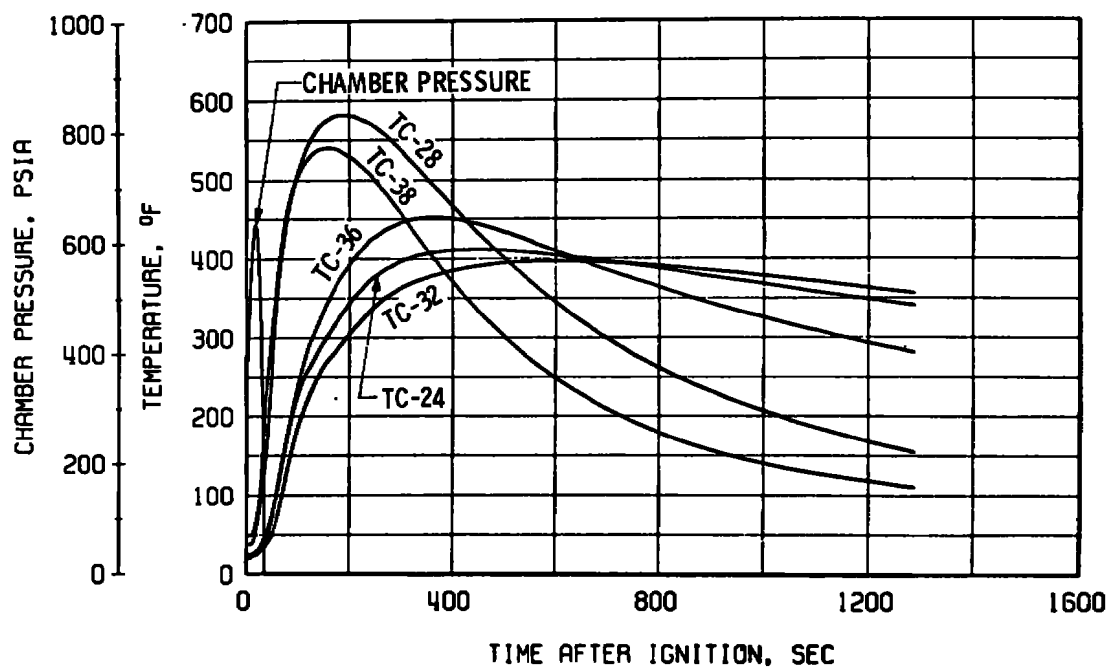


r. Exhaust nozzle (Q3)

Figure 7. Continued.

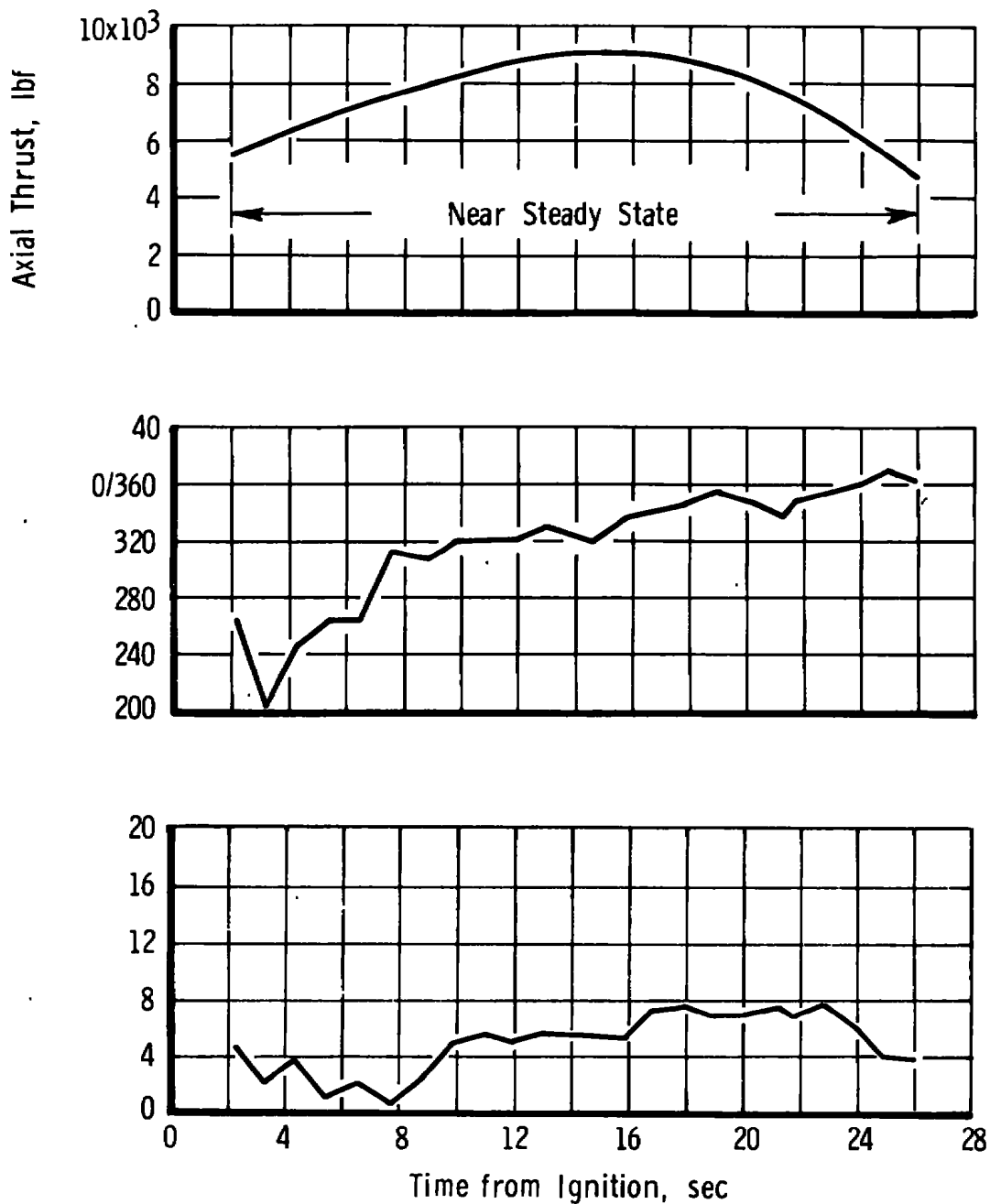


s. Exhaust nozzle (Q3)



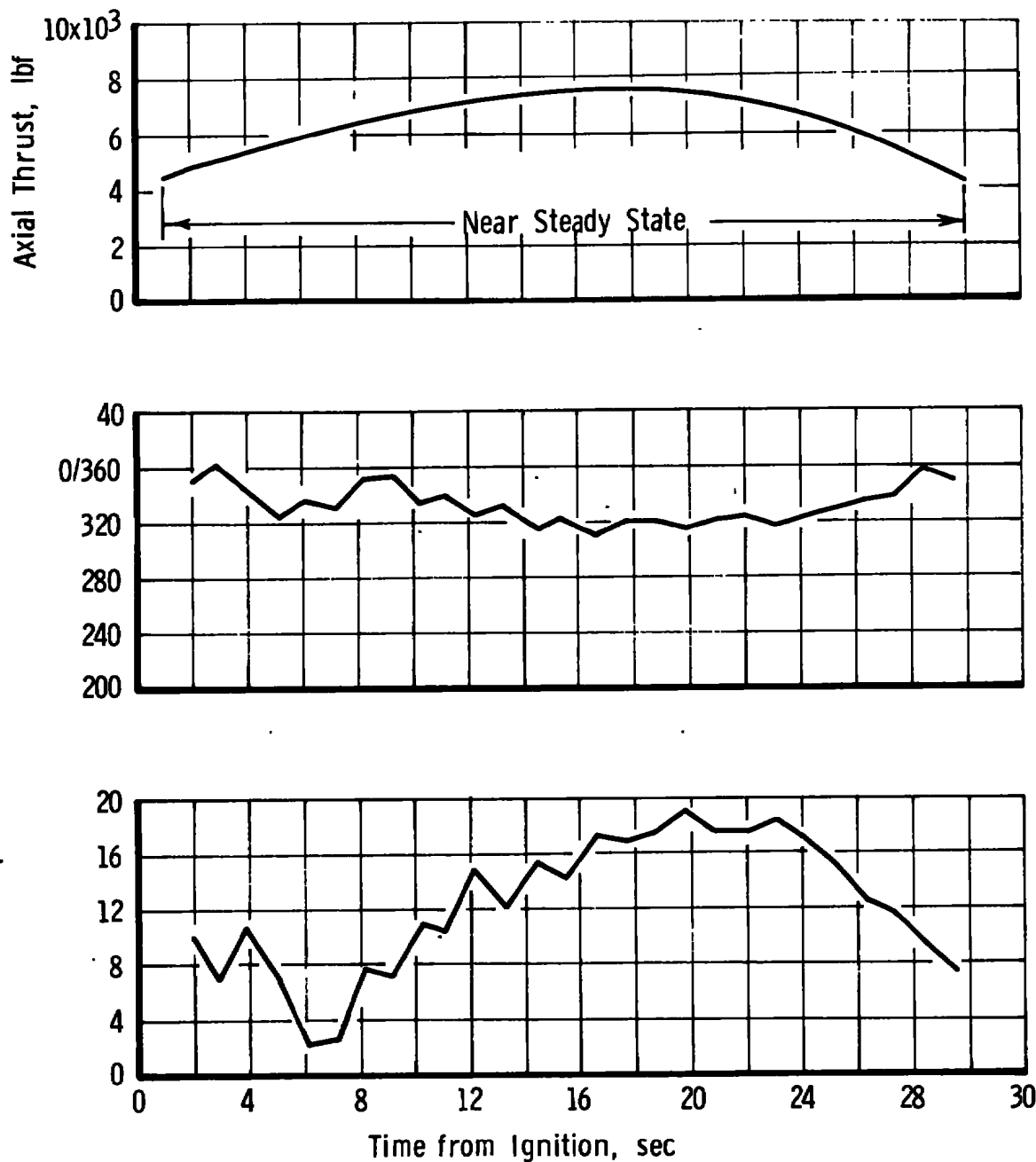
t. Exhaust nozzle (Q3)

Figure 7. Concluded.



a. Motor Q2

Figure 8. Variation in the lateral (nonaxial) component of the thrust vector during firing.



b. Motor Q3
Figure 8. Concluded.

Table 1. Instrumentation Summary and Measurement Uncertainty

Parameter Designation	STEADY-STATE ESTIMATED MEASUREMENT*							Range	Type of Measuring Device	Type of Recording Device	Method of System Calibration	
	Precision Index (S)			Bias (B)		Uncertainty $\pm(B + 1.95S)$						
	Percent of Reading	Unit of Measurement	Degree of Freedom	Percent of Reading	Unit of Measurement	Percent of Reading	Unit of Measurement					
Axial Force, lbf	± 0.09	----	117	± 0.06	----	± 0.24	----	4900 to 9200 lbf	Bonded Strain-Gage-Type Force Transducers	Sequential Sampling, Millivolt-to-Digital Converter, and Magnetic Tape Storage Data Acquisition System	In-Place Application of Deadweights Calibrated in the Standards Laboratory	
Total Impulse, lbf-sec	± 0.09	----	117	± 0.07	----	± 0.25	----	----	↓			
Chamber Pressure, psia	± 0.2	----	39	± 0.2	----	± 0.6	----	420 to 800 psia	Strain-Gage-Type Pressure Transducer		↓	In-Place Application of Voltage Levels Measured with a Voltmeter Calibrated in the Standards Laboratory
Chamber Pressure Integral, psia-sec	± 0.2	----	39	± 0.2	----	± 0.6	----	----	↓			
Test Cell Pressure, psia	± 0.2	----	39	± 1.7	----	± 2	----	0.06 to 0.90 psia	Unbonded Strain-Gage-Type Pressure Transducers		↓	Resistance Shunt Based on the Standards Laboratory Determination of Transducer Applied Pressure versus Resistance Shunt Equivalent Pressure Relationship
Test Cell Pressure Integral, psia-sec	± 0.2	----	39	± 1.7	----	± 2	----	----	↓			
Temperature, °F	----	$\pm 0.6^{\circ}\text{F}$	191	----	$\pm 0.9^{\circ}\text{F}$	----	$\pm 2^{\circ}\text{F}$	70 to 200°F	Chromel-Alumel Temperature Transducers	↓	Millivolt Substitution Based on the NBS Temperature versus Millivolt Tables	
	----	$\pm 0.6^{\circ}\text{F}$	191	$\pm(0.25\% + 0.4^{\circ}\text{F})$		$\pm(0.25\% + 1.6^{\circ}\text{F})$		200 to 800°F				
Weight, lbm	----	± 0.015 lbm	31	----	± 0.052 lbm	----	± 0.08 lbm	570 to 1300 lbm	Beam Balance Scales	Visual Readout	In-Place Application of Deadweights Calibrated in the Standards Laboratory	
Fwd Dome Growth, Inches	± 1.5	----	31	± 1.0	----	± 4	----	0.120 to 0.350 in.	Rectilinear Potentiometer	Sequential Sampling, Millivolt-to-Digital Converter, and Magnetic Tape Storage Data Acquisition System	In-Place Application of Multiple Gage Blocks Calibrated in the Standards Laboratory	
Lateral Thrust Vector Magnitude, lbf	----	± 1 lbf	44	----	± 1 lbf	----	± 3 lbf	2.0 to 20.0 lbf	Bonded Strain-Gage-Type Force Transducers		↓	In-Place Application of Multiple Force Levels Measured with Force Transducers in the Standards Laboratory

*REFERENCE: CPFA No. 180, "ICRPG Handbook for Estimating the Uncertainty in Measurements made with Liquid Propellant Rocket Engine Systems," (AD655130), April 30, 1969.

Table 2. Summary of SVM-6 Motor Performance

			Specification ^a <u>Limits</u>
Test Number R41C-26A	01	02	
Motor Serial Number	Q2	Q3	
Test Date	5/23/75	6/20/75	
Motor Spin Rate During Firing, rpm	112	111	
Average Motor Case Temperature at Ignition, °F	109	18	
Ignition Time, (t _i) ¹ , sec	0.031	0.038	< 0.185
Action Time (t _a) ² , sec	29.037	34.353	< 43 sec @ 55°F
Total Burn Time (t _t) ³ , sec	35.905	40.578	
Simulated Altitude at Ignition, ft	113,000	123,000	
Average Simulated Altitude During t _a , ft	82,000	83,000	
Measured Total Impulse (based on t _t), lbf-sec	204,578	203,695	
Number of Data Channels Averaged	4	4	
Maximum Channel Deviation from Average, percent	0.13	0.05	
Chamber Pressure Integral (based on t _t), psia-sec	17,691	17,502	
Cell Pressure Integral (based on t _t), psia-sec	15.026	14.093	
Number of Data Channels Averaged	2	2	
Maximum Channel Deviation from Average, percent	0.27	0.26	
Maximum Chamber Pressure, psia	786	647	
Maximum Measured Thrust, lbf	9188	7597	
Vacuum Total Impulse (based on t _a), lbf-sec	208,042	207,588	
Vacuum Total Impulse (based on t _t), lbf-sec	208,433	208,474	208,425 to 211,575
Vacuum Specific Impulse (based on t _a), lbf-sec/lbm			
Based on Manufacturer's Stated Propellant Weight	294.42	292.47	
Based on Expended Mass (AEDC)	290.65	288.54	
Vacuum Specific Impulse (based on t _t), lbf-sec/lbm			
Based on Manufacturer's Stated Propellant Weight	294.97	293.72	
Based on Expended Mass (AEDC)	291.20	289.77	

¹Ignition time is the time interval from application of ignition voltage until axial thrust reaches 75 percent of maximum thrust during ignition.

²Action time is the time interval beginning when chamber pressure has risen to 10 percent of maximum chamber pressure and ending when chamber pressure has fallen to 10 percent of maximum chamber pressure during tailoff.

³Total burn time is the time interval from application of ignition voltage until chamber pressure decreases to cell pressure at burnout.

^aProduct Specification for Solid Propellant Apogee Kick Motor, AS311332, Code 09205 Rev. E, dated September 11, 1974, Philco-Ford Corporation, Newport Beach, California

Table 3. Summary of SVM-6 Motor Physical Dimensions

Test Number, R41C-26A	01	02
Motor Serial Number	Q2	Q3
Test Date	5-23-75	6-20-75
Motor Spin Rate, rpm	112	111
AEDC Prefire Motor Weight, ¹ lbm	1292.83	1293.24
AEDC Postfire Motor Weight, ¹ lbm	577.05	573.79
AEDC Expended Mass, lbm	715.78	719.45
Manufacturer's Stated Propellant Weight, lbm	706.62	709.77
Nozzle Throat Area, in. ²		
Prefire	6.335	6.338
Postfire	6.007	6.089
Percent Change from Prefire	-5.12	-3.93
Nozzle Exit Area, in. ²		
Prefire	337.251	337.561
Postfire	339.990	340.613
Percent Change from Prefire	+0.81	+0.90

¹NOTE: Includes weight of firing harness.

NOMENCLATURE

- t_a Action time, the time interval beginning when chamber pressure has risen to 10 percent of maximum chamber pressure and ending when chamber pressure has fallen to 10 percent of maximum chamber pressure during tailoff
- t_i Ignition time, the time interval from application of ignition voltage until axial thrust reaches 75 percent of maximum thrust during ignition
- t_T Total burn time, the time interval from application of ignition voltage until chamber pressure decreases to cell pressure at burnout